VECTOR CONTROL OF TWO-LEVEL VOLTAGE SOURCE INVERTER (VSI) FED 3-PHASE INDUCTION MOTOR

A project Report

Submitted by

SURYA KUMAR BEHERA

In partial fulfillment of the requirements for the award of the degree of

MASTER OF TECHNOLOGY

IN

CONSTRUCTION TECHNOLOGY AND MANAGEMENT

BUILDING TECHNOLOGY AND CONSTRUCTION MANAGEMENT

DEPARTMENT OF CIVIL ENGINEERING

INDIAN INSTITUTE OF TECHNOLOGY MADRAS

MAY 2015

CERTIFICATE

This is to certify that the thesis titled **"VECTOR CONTROL OF TWO-LEVEL VOLTAGE SOURCE INVERTER (VSI) FED 3-PHASE INDUCTION MOTOR"** submitted by **SURYA KUMAR BEHERA** (CE13M177), to the **Indian Institute of Technology Madras**, in partial fulfilment of the requirements for the award of the degree of **MASTER OF TECHNOLOGY** in Construction Technology and Management is a bonafide record of work carried by him under my supervision. The contents of this thesis, in full or in parts, have not been submitted and neither will be submitted to any other Institute or University for the award of any degree or diploma.

Dr. Srirama Srinivas
Associate Professor
ESB-208A, Dept. of Electrical Engg.
Indian Institute of Technology Madras
Chennai-600 036, TN
INDIA.
Ph: +91 44 22574447 (O)
Fax: +91 44 22574402

Dr. A. Meher Prasad
Professor and Head
Department of Civil Engineering
IIT Madras

Place: Chennai

Date: 06th May 2015

ACKNOWLEDGEMENTS

First, and foremost, I thank Almighty for blessing me with strength and courage to complete my research work. I thank my parents for their unconditional love, patience, affection and support for everything I had attempted to do throughout my life.

I would like to express my reverential gratitude to my project guide **Dr. Srirama Srinivas**, Associate Professor, Dept. of Electrical Engg., Indian Institute of Technology Madras, for his continuous support, motivation and guidance throughout the project. It was a great learning experience to work with him, and I thank him for giving me the opportunity.

I am deeply indebted to my L&T guide **Mr. Samaresh Bhattacharya**, CHIEF ENGINEERING MANAGER (ELEC), EDRC-KOLKATA (M&M)**,** L&T Construction, for his insightful guidance and giving constant enthusiasm and support to my research work. I am grateful for his time, efforts during my summer training.

I am grateful to Dr. Kamlesh Hatua, Associate Professor, Dept. of Electrical Engg., Indian Institute of Technology Madras and Professor **Dr. K. Ananthanarayanan**, Co-ordinator, M.Tech Construction Technology and Management course, Indian Institute of Technology Madras, for offering me constructive comments and suggestions at various stages of my study.

I am also thankful to my classmates and friends Ms. Hridya Ittamveettil, Mr. Saikat Kumar Jana for giving me valuable suggestions and ideas throughout my project work.

Finally I thank all the members of the M.Tech Construction Technology and Management (2012-2014) and M.Tech Building Technology and Construction Management (2012-2014) family for making my stay in IIT-Madras, a memorable one filled with lot of good memories.

SURYA KUMAR BEHERA

ABSTRACT

KEYWORDS: *Vector Control, Simulink, SPWM, dSPACE*.

In today's world, induction motor is most widely used motor due to number of reasons such as good self-starting capability, simple and rugged structure, low cost and reliability, etc. However, it does not have the capability of variable speed operation inherently like DC machines. Because of this reason, DC motors were used in most of the applications where variable speed operation was required. But recent developments in DC motor like speed control techniques for the AC machines have led to their large scale use in most of the electrical drives.

The concept of vector control (field oriented control) has made it very clear that AC motors can be controlled to achieve fast speed dynamic performance as good as that of DC motors. In order to understand and analyze vector control, the dynamic model of the induction motor is necessary.

Research shows that dynamic model developed on a rotating reference frame is easier to describe the dynamic or transient characteristics of induction motors because at synchronous speed reference frame the rotating magnetic flux appears as DC quantity. So the main objective of the project to derive and explain induction motor model in relatively simple terms by using the concept of space vectors, α-β & d-q transformation. It is seen that when we choose synchronous reference frame in which rotor flux lies on the d-axis, dynamic equations of the induction motor are simplified and appear similar to that of a separated excited DC motor.

Analysis has been done on a three phase squirrel cage induction motor of 1.1 KW rating. Machine modelling is performed in rotor flux frame to analyze the dynamic performance of the motor using MATLAB-Simulink. Indirect vector control is employed with sine-PWM technique and starting performance, load disturbance and speed reversal characteristics are observed in Simulink. Finally the whole system is implemented on a laboratory prototype hardware system using d-Space as digital platform.

TABLE OF CONTENTS

LIST OF TABLES

LIST OF FIGURES

ABBREVIATIONS

FOC	Field Oriented Control
VC	Vector Control
IM	Induction Motor
DTC	Direct Torque Control
RPS	Radian per second
RPM	Rotation per minute
PWM	Pulse Width Modulation
VSI	Voltage Source Inverter
SPWM	Sine wave Pulse Width Modulation

NOTATIONS AND SYMBOLS

V_s	Voltage space vector
I_s	Current space vector
V	Voltage
F	Frequency
d^e-q^e	Synchronously rotating reference frame direct & quadrature axis
α-β	Stationary reference frame direct & quadrature axes
V_a	α -axis component of voltage space vector
V_b	β -axis component of voltage space vector
I_s	Rms Stator Current
I_r	Rms Rotor current
i_{qs}	q-axis stator current
i_{ds}	d-axis stator current
J	Moment of inertia (Kg-m^2)
B	Friction Constant
X_r	Rotor reactance (ohm)
X_s	Synchronous reactance (ohm)
X_{lr}	Rotor leakage reactance
X_{ls}	Stator leakage reactance
θ_r	Rotor Angle
θ_{sl}	Slip angle
L_m	Magnetizing Inductance
L_r	Rotor Inductance
L_s	Stator Inductance
L_{lr}	Rotor leakage Inductance
L_{ls}	Stator leakage Inductance
R_r	Rotor resistance (Ohm)
R_s	Stator resistance (Ohm)
S	Slip
M_d	Developed Torque
M_L	Load Torque
V_{dc}	Dc-link voltage
ψ_r	Rotor flux linkage
ψ_s	Stator flux linkage
ψ_m	Air gap flux linkage
w_m	Rotor mechanical speed (rad/s)
w_{mr}	Stator line frequency/synchronous frequency (rad/s)
w_r	Rotor electrical speed
w_{sl}	Slip frequency
T_s	Sampling time period

CHAPTER 1

INTRODUCTION

1.1. BASICS OF FIELD ORIENTED CONTROL

V/f speed control or scalar control is easy to implement, however it gives sluggish or inferior response due to inherent coupling effect i.e. both torque and flux are functions of voltage or current & frequency, which leads to poor speed dynamic response.

This particular problem can be solved by vector control or field oriented control technique. Here, a three phase motor can be operated as separately excited dc motor where torque & flux component of stator current are independent of each other, hence total decoupling is achieved.

In a separately excited dc motor, neglecting armature reaction & field saturation, the developed torque is given as

$$T_e = K_t\, i_a\, i_f \quad \ldots\ldots\ldots\ldots\ldots\ldots\ldots\ldots\ldots\ldots\ldots\ldots\ldots\ldots (1.1)$$

Where i_a is armature current & i_f is field current, both this currents are perpendicular to each other, in other words these quantities are orthogonal to each other & also are stationary in space. As shown in fig 1.1(a) if torque is controlled by i_a , then the flux is not effected. But in induction motor, this type of control is not possible due to inherent coupling problem, resulting in large speed dynamics.

Vector control is based on synchronously rotating reference frame (d-q), where sinusoidal variables appear as dc quantities in steady state.

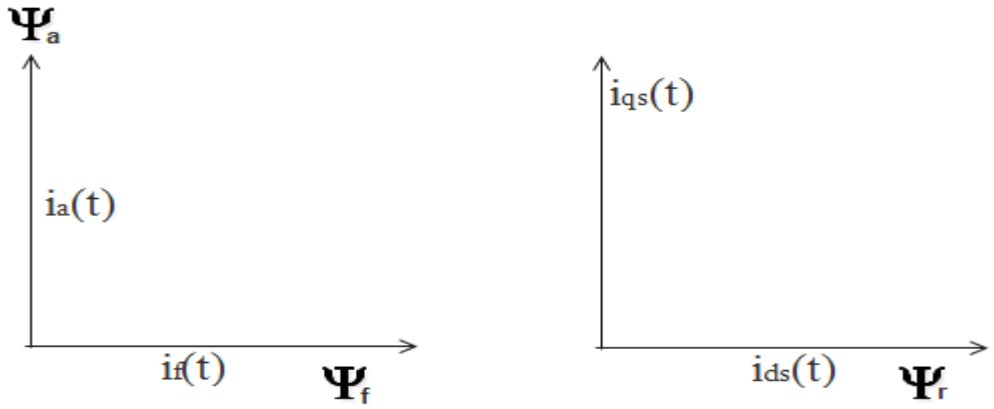

Fig 1.1: (a) separately excited dc motor (b) vector controlled induction motor

Here i_{qs} & i_{ds} are quadrature axis & direct axis component of stator current respectively in synchronously rotating reference frame. So for 3 phase induction machine torque can be expressed as

$$T_e = K_i \, i_{qs} \, i_{ds} \quad \ldots\ldots\ldots\ldots\ldots\ldots\ldots\ldots\ldots\ldots\ldots\ldots\ldots \text{(1.2)}$$

In vector control technique, torque is controlled by varying i_{qs}, where as i_{ds} is kept constant as shown in fig 1.1(b).

Various advantages of using vector control are listed below:

a) Decoupled control of torque and flux.
b) Better speed dynamic response.
c) Fast speed response.
d) Four quadrant operation.

1.2. CONCEPT OF V/F CONTROL & DTC AS COMPARED TO VECTOR CONTROL (FOC)

1.2.1. Scalar Control (V/f control)

Open loop volts/Hz control or V/f control was most popular speed control technique. Because of its simplicity & low cost, it is widely used in industries. In an induction motor to change the speed, we need to change the frequency. But to keep the flux of the machine constant, we need to change the voltage of the machine proportionally with change in frequency.

Disadvantages of scalar control:

- Due to inherent coupling effect the torque response is slow.
- At lower frequencies, there is some amount of underdamping in torque & flux responses. However, speed response does not get affected due to inertia.
- Drift in flux for varying torque.
- System is prone to instability due to fifth-order system effect.

1.2.2. Direct Torque Control (DTC)

The principle of DTC is to control directly the stator flux & torque of an induction machine by applying the appropriate stator voltage space vector. This control techniques eliminates almost all the drawbacks of scalar control or v/f control. It has high torque dynamics as compared to vector control or FOC. However it has some drawbacks which are listed below:

- Higher torque ripple.
- Variable switching frequency.

1.3. DSPACE-AN OVERVIEW

Due to the complex mathematical calculations involved in vector control technique, it requires continuous processing of all the data at high speed. The feedback signal processing, feed-forward calculation, axes transformation requires a fast, accurate & effective control hardware. For this project dSPACE was used for continuous digital signal processing.

The DS1104 R&D Controller Board is a standard board that can be plugged into a PCI slot of a PC. The DS1104 is specifically designed for the development of high-speed multivariable digital controllers and real-time simulations in various fields. It is a complete real-time control system based on a 603 PowerPC floating-point processor running at 250 MHz, for advanced I/O purposes. The board includes a slave-DSP subsystem based on the TMS320F240 DSP microcontroller.

1.4. OBJECTIVES

The objectives defined for this study are as follow:

- To develop a closed loop speed control system for induction motor.
- To develop a three phase induction motor model.
- Design of Sine PWM- modulator for a Voltage Source Inverter (VSI).
- Design of speed, current and flux controllers.
- Validation on a laboratory prototype module consisting of the above motor drive system.

1.5. SCOPE

This project covers several academic areas, such as computer architecture, analog and digital circuit design and construction, induction machine modeling and vector control theory with the representation of three-phase quantities in the complex plane. Analysis had been done for a three phase squirrel cage induction motor of 1.1 KW rating. Machine modelling was performed in rotor flux frame to analyze the dynamic performance of the motor using MATLAB-Simulink. The vector control system is first designed on-paper as a continuous time system and it is verified with the simulation using Matlab/Simulink. The electrical interfaces, analog and digital, are designed according to the application circuits in the selected components' data sheets.

1.6. ORGANISATION OF THE THESIS

This report consists of eight chapters including this chapter. The content of each of the chapters is discussed as follows:

Chapter 2 – This chapter gives basic idea of space phasor concept & how it is helpful in studying dynamic behavior of three phase machines. All the equations required for vector control in rotor flux reference are derived step by step.

Chapter 3 – Various types of vector control techniques are discussed briefly & all equation & axes transformation equations are summarized.

Chapter 4 – This chapter explains MATLAB Simulink model of 3 phase induction motor. All the output waveforms are analyzed briefly.

Chapter 5 – This chapter explains MATLAB Simulink model of indirect vector control. All the output waveforms are discussed & analyzed briefly. Controller design method is described in detail & sine PWM technique is also discussed.

Chapter 6 –This chapter contains the details of development of a framework for addressing the various major interface issues while undergoing hardware implementation. It also presents experimental setup & hardware results.

Chapter 7–This chapter contains the summary of the thesis and also the major conclusions drawn from this study.

CHAPTER 2

SPACE PHASOR CONCEPT

2.1. INTRODUCTION

The space-vector concept is used to study the dynamic or transient speed response of the AC motors. In space-vector theory, the following assumptions are taken to simplify the analysis:

- the flux density distribution is assumed sinusoidal in the air gap,
- the saturation of the magnetizing circuit is assumed constant,
- there are no iron loss or copper loss.
- the resistances and inductances are independent of the temperature and frequency

Let us consider there phase windings of an AC machine similar to the stator winding of an induction motor. Fig 2.1 shows the schematic diagram of the three phase coils, each of which has Ns turns and electrically 120 degree phase displaced.

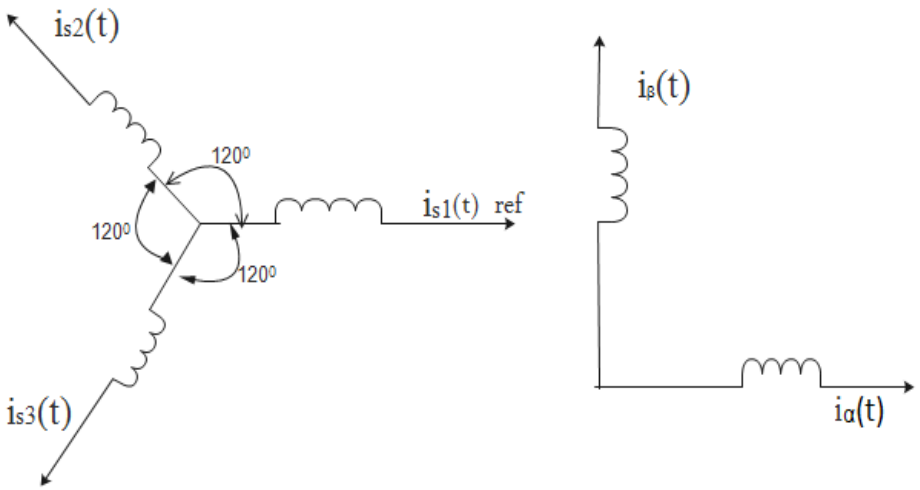

Fig 2.1: (a) Schematic diagram of three phase coils

(b) Net current component along $\alpha-\beta$ axis

The flux density distribution was assumed sinusoidal. Again due to isolated neutral, it can be stated that:

$$i_{s1}(t) + i_{s2}(t) + i_{s3}(t) = 0 \quad \text{..... (2.1)}$$

Now the net MMF can be resolved into two orthogonal components i.e. component along the reference axis (coil-1 direction) and perpendicular to it as shown in Fig 2.1(b).

If these components are denoted by subscripts α and β respectively, then it can be written as:

$$MMF_\alpha = N_s * \left(i_{s1}(t) - \left(\frac{1}{2}\right) i_{s2}(t) - \left(\frac{1}{2}\right) i_{s3}(t)\right) = N_s * (\frac{3}{2}) i_{s1}(t) \ldots\ldots (2.2)$$

$$MMF_\beta = N_s * \left(\frac{\sqrt{3}}{2}\right) (i_{s2}(t) - i_{s3}(t)) \ldots\ldots (2.3)$$

$$\& \text{ Net } MMF = N_s(i_{s1}(t)\ e^{j0} + i_{s2}(t)e^{j120} + i_{s3}(t)e^{j240}) \ldots\ldots (2.4)$$

We can also write it in current form, i.e.

$$i_{s\alpha} = (\frac{3}{2}) i_{s1}(t) \ldots\ldots (2.5)$$

$$i_{s\beta} = \left(\frac{\sqrt{3}}{2}\right) (i_{s2}(t) - i_{s3}(t)) \ldots\ldots (2.6)$$

So current space phasor $\tilde{\imath}_s$ can be expressed as

$$\tilde{\imath}_s(t) = i_{s\alpha}(t) + j\, i_{s\beta}(t) \ldots\ldots (2.7)$$

The above equations are true for current, voltage and flux linkages.

2.2. SINOSOIDAL STEADY-STATE OPERATION

If $i_{s1}(t) = i_m\, Cos\, (wt)$

$i_{s2}(t) = i_m Cos\, (wt - 120)$

$i_{s3}(t) = i_m Cos\, (wt + 120)$

Then $\tilde{\imath}_s(t) = i_{s1}(t)\ e^{j0} + i_{s2}(t)e^{j120} + i_{s3}(t)e^{j240}$

$$= (3/2) * i_m * e^{jwt} \ldots\ldots (2.8)$$

2.3. INDUCTION MACHINE EQUATION IN SPACE PHASOR FORM

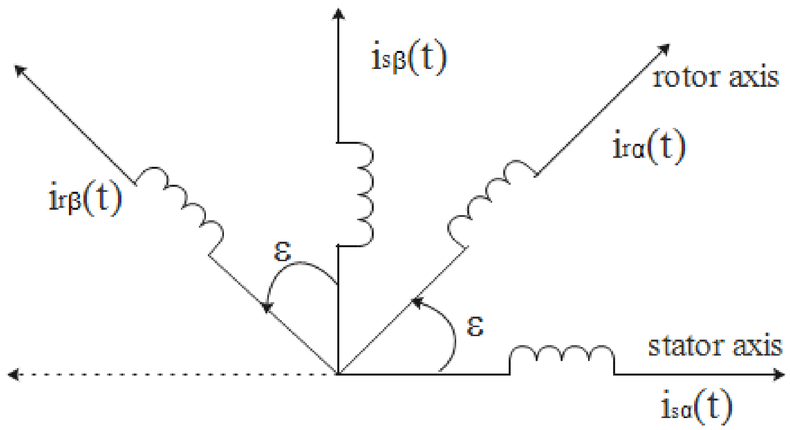

Fig 2.2: Stator & rotor current phasors along $\alpha-\beta$ axis

In Fig 2.2, it is shown that the two three phase coils of the induction motor, i.e. stator and rotor winding, can be represented as two equivalent two phase coils.

If the rotor axis makes an angle ε(t) w.r.t the stator axis, the current space phasors $i_s(t)$ and $i_r(t)$ can be written as:

$\tilde{\imath}_s(t) = i_{s\alpha}(t) + j\, i_{s\beta}(t)$ ……In stator coordinates

$\tilde{\imath}_r(t) = i_{r\alpha}(t) + j\, i_{r\beta}(t)$ ……..…….. In rotor coordinates

Flux linkages in α-β frame will be

$\psi_{s\alpha}(t) = L_s i_{s\alpha}(t) + M\, i_{r\alpha}(t)\, cos\, \varepsilon(t) - M\ \ i_{r\beta}(t) \sin\ \varepsilon(t)$…….……..…. (2.9)

$\psi_{s\beta}(t) = L_s i_{s\beta}(t) + M\, i_{r\alpha}(t)\, sin\, \varepsilon(t) + M\ \ i_{r\beta}(t) \cos\ \varepsilon(t)$ ……. (2.10)

Combining (2.9) and (2.10), the stator flux space phasor will be

$\tilde{\Psi}_s(t) = \psi_{s\alpha}(t) + j\, \psi_{s\beta}(t) = L_s \tilde{\imath}_s(t) + M\, \tilde{\imath}_r(t)\, e^{j\varepsilon(t)}$…….……..…… (2.11)

Similarly the rotor flux phasor will be

$\tilde{\Psi}_r(t) = \psi_{r\alpha}(t) + j\, \psi_{r\beta}(t) = L_r \tilde{\imath}_r(t) + M\, \tilde{\imath}_s(t)\, e^{-j\varepsilon(t)}$……...……. (2.12)

Where

L_s = self-inductance of stator coil

L_r = self-inductance of rotor coil

M = L_o= mutual inductance between stator and rotor coil

(2.11) is w.r.t stator coordinate and (2.12) is w.r.t rotor coordinates & it is assumed that multiplication by $e^{j\varepsilon(t)}$ results in a clockwise rotation of the coordinate system by an angle ε(t), while multiplication by $e^{-j\varepsilon(t)}$ results in anticlockwise rotation of the coordinate system by the same angle.

Now voltage-current equation for the stator and rotor windings can be written in α-β frame as:

$$\mathbf{v}_{s\alpha}(t) = R_s i_{s\alpha}(t) + \frac{d\Psi_{s\alpha}(t)}{dt}$$

$$\mathbf{v}_{s\beta}(t) = R_s i_{s\beta}(t) + \frac{d\Psi_{s\beta}(t)}{dt}$$

$$\mathbf{v}_{r\alpha}(t) = R_s i_{r\alpha}(t) + \frac{d\Psi_{r\alpha}(t)}{dt}$$

$$\mathbf{v}_{r\beta}(t) = R_s i_{r\beta}(t) + \frac{d\Psi_{r\beta}(t)}{dt}$$

Where

R_s =stator resistance, R_r = rotor resistance

Combining above equations, we obtain two complex equations as follows:

$$\tilde{\mathbf{v}}_s(t) = R_s \tilde{i}_s(t) + \frac{d\tilde{\Psi}_s(t)}{dt} \quad \text{..................................... (2.13)}$$

$$\tilde{\mathbf{v}}_r(t) = R_r \tilde{i}_r(t) + \frac{d\tilde{\Psi}_r(t)}{dt} \quad \text{..................................... (2.14)}$$

Putting (2.11) & (2.12) in above equations, these can be rewritten as

$$\tilde{\mathbf{v}}_s(t) = R_s \tilde{i}_s(t) + L_s \frac{d\,\tilde{i}_s(t)}{dt} + M \frac{d\,(\tilde{I}_r(t)e^{j\varepsilon(t)})}{dt} \quad \text{.................... (2.15)}$$

$$\tilde{\mathbf{v}}_r(t) = 0 = R_r \tilde{i}_r(t) + L_r \frac{d\,\tilde{i}_r(t)}{dt} + M \frac{d\,(\tilde{i}_s(t)e^{-j\varepsilon(t)})}{dt} \quad \text{............ (2.16)}$$

(2.15) is in stator coordinates whereas (2.16) is in to rotor coordinates. The torque developed by the machine is given as:

$$M_d = \frac{2}{3}\,\frac{P}{2}\,M\,I_m[\,\tilde{\imath}_s(t)\,\{\tilde{\imath}_r(t)\,e^{j\varepsilon(t)}\}^*\,] \quad \text{........................ (2.17)}$$

Where I_m stands for imaginary part and * denotes complex conjugate, P is no of poles in the concerned machine. Again in terms of inertia and load torque, it can be written as

$$J\frac{dw_m}{dt} + Bw_m = M_d - M_l \quad \text{....................................... (2.18)}$$

$$\frac{P}{2}w_m = w_r = \frac{d\varepsilon(t)}{dt} \quad \text{.. (2.19)}$$

Where

w_m= rotor speed in mechanical rad/sec

w_r= rotor speed in electrical rad/sec

J = moment of inertia

M_l= Load torque

2.4. DYNAMICS OF INDUCTION MOTOR IN THE ROTOR FLUX FRAME OF REFERENCE

(2.15) (i.e. stator equation in stator frame) serves to determine the stator voltage $\tilde{v}_s(t)$ in synchronously rotating rotor flux frame (i.e. v_{ds} & v_{qs}). (2.16) (i.e. rotor equation in rotor frame) is used to derive the dynamic equations to describe the mechanical behavior of the induction machine.

2.4.1. Stator equation

From (2.15)

$$\tilde{\mathbf{v}}_s(t) = R_s \tilde{i}_s(t) + L_s \frac{d\,\tilde{i}_s(t)}{dt} + M \frac{d\ (\tilde{I}_r(t) e^{j\varepsilon(t)})}{dt} \quad \ldots\ldots \text{(In stator reference frame)}$$

From the steady state model of induction motor,

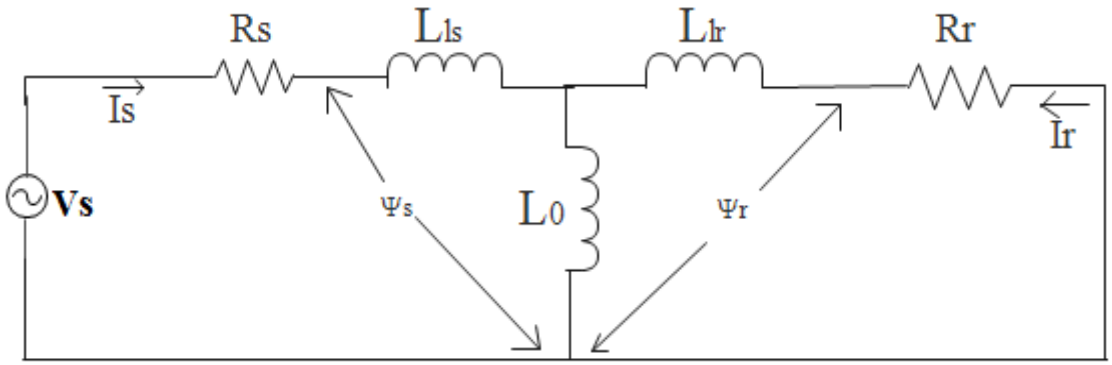

Fig 2.3: Induction motor in steady state

$\Psi_r{}^r = \Psi_{lr} + \Psi_o$

$= L_{lr}\, i_r + L_o\,(i_s + i_r)$

$= (L_{lr} + L_o)\, i_r + L_o\, i_s$

$= L_r\, i_r + L_o\, i_s = (\sigma_r + 1) L_o i_r + L_o\, i_s$

Here $\Psi_r{}^r$ is in rotor frame of reference. Now $\Psi_r{}^r$ is in stator frame of reference will be as

$$\Psi_r{}^s = (\sigma_r + 1)L_o i_r e^{j\varepsilon} + L_o\, i_s$$

$$= [(\sigma_r + 1) i_r e^{j\varepsilon} + i_s] L_o$$

$$= i_{mr}{}^* L_o$$

Where

L_o = Mutual Inductance

L_{lr} = Leakage-inductance of rotor

$L_r = L_{lr} + L_o$ = Rotor self-inductance

If $\sigma_r = \frac{L_{lr}}{L_o}$, $L_r = (\sigma_r + 1)L_o$

$$\sigma = 1 - \frac{L_o{}^2}{L_s * L_r}$$

Where

$$i_{mr}{}^s = [(\sigma_r + 1) i_r e^{j\varepsilon} + i_s] \quad \text{..... (2.20)}$$

$$\Rightarrow i_r e^{j\varepsilon} = \frac{i_{mr}{}^s - i_s}{\sigma_r + 1} \quad \text{..... (2.21)}$$

Putting (2.21) in (2.15)

$$\tilde{\mathbf{v}}_s(t)^s = R_s \tilde{\imath}_s(t) + L_s \frac{d\,\tilde{\imath}_s(t)}{dt} + L_o \frac{d}{dt}\left\{\frac{\tilde{\imath}_{mr}{}^s - \tilde{\imath}_s}{\sigma_r + 1}\right\}$$

$$= R_s \tilde{\imath}_s(t) + \sigma L_s \frac{d\,\tilde{\imath}_s(t)}{dt} + L_s(1-\sigma)\frac{d\,\tilde{\imath}_{mr}{}^s}{dt} \quad \text{..... (2.22)}$$

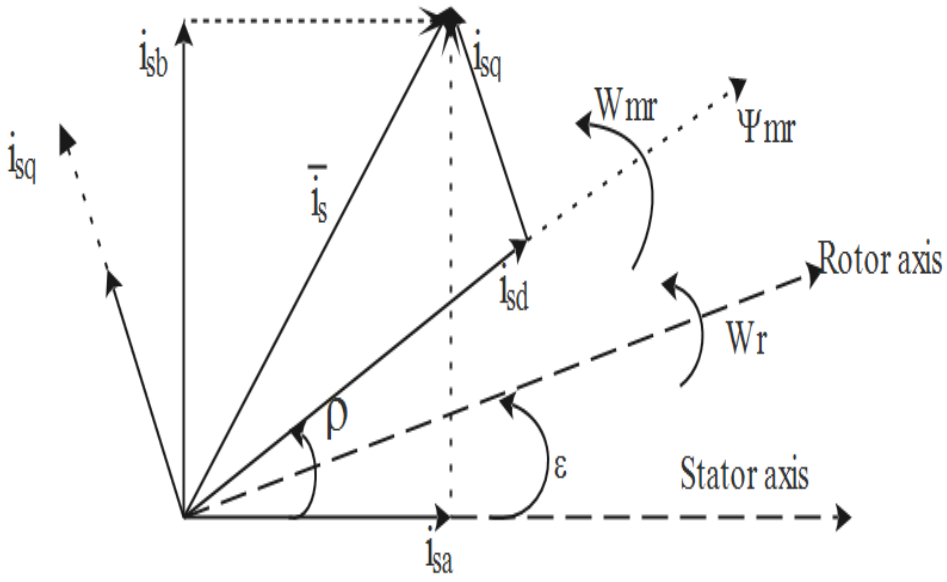

Fig 2.4: Spatial orientation of different fluxes

Now (2.22) can be rewritten as

$$\tilde{\mathbf{v}}_s(\mathrm{t})^{\rho} * e^{j\rho(t)} = R_s * \tilde{\imath}_s(\mathrm{t})^{\rho} * e^{j\rho(t)} + \sigma L_s \frac{d\{\tilde{\imath}_s(\mathrm{t})^{\rho} * e^{j\rho(t)}\}}{dt}$$

$$+ L_s(1-\sigma)\frac{d\{\tilde{\imath}_{mr}{}^{\rho} * e^{j\rho(t)}\}}{dt} \ldots\ldots\ldots\ldots\ldots\ldots \text{(2.23)}$$

Taking $\tilde{\mathbf{v}}_s(\mathrm{t})^{\rho} * e^{j\rho(t)} = v_{ds} + \mathrm{j}v_{qs}$

$$\tilde{\imath}_s(\mathrm{t})^{\rho} * e^{j\rho(t)} = i_{ds} + \mathrm{j}i_{qs}$$

$$w_{mr} = \frac{d\rho(t)}{dt} \ldots\ldots\ldots\ldots\ldots\ldots\ldots\ldots\ldots\ldots \text{(2.24)}$$

(2.23) can be separated into real and imaginary parts as follows:

$$v_{ds} = R_s\, i_{ds} - \sigma\, L_s i_{qs} w_{mr} + \sigma\, L_s \frac{di_{ds}}{dt} + (1-\sigma)\, L_s \frac{di_{mr}}{dt} \ldots\ldots\ldots \text{(2.25)}$$

$$v_{qs} = R_s\, i_{qs} + \sigma\, L_s i_{ds} w_{mr} + \sigma\, L_s \frac{di_{qs}}{dt} + (1-\sigma)\, L_s i_{mr} w_{mr} \ldots\ldots \text{(2.26)}$$

2.4.2. Rotor equation

(2.16) can be written as

$$\tilde{\mathbf{v}}_r(\mathrm{t}) = 0 = R_r \tilde{\imath}_r(\mathrm{t}) + L_r \frac{d\,\tilde{\imath}_r(\mathrm{t})}{dt} + \mathrm{M}\frac{d(\tilde{\imath}_s(\mathrm{t}) * e^{-\mathrm{j}\varepsilon(\mathrm{t})})}{dt} \ldots\ldots \text{(In rotor reference frame)}$$

From (2.12)

$$\tilde{\Psi}_r(\mathrm{t})^r = \psi_{ra}(\mathrm{t}) + \mathrm{j}\,\psi_{rb}(\mathrm{t}) = L_r \tilde{\imath}_r(\mathrm{t}) + \mathrm{M}\,\tilde{\imath}_s(\mathrm{t})\; e^{-\mathrm{j}\varepsilon(\mathrm{t})}$$

$$= (\sigma_r + 1) L_o \tilde{\imath}_r(t) + L_o\, \tilde{\imath}_s(t) e^{-j\varepsilon(t)}] = \{(\sigma_r + 1)\tilde{\imath}_r(t) + \tilde{\imath}_s(t) e^{-j\varepsilon(t)}\} * L_o$$

The above equation is in rotor axis frame, so bringing it in stator axis frame

$$\tilde{\Psi}_r(\mathrm{t})^r * e^{j\varepsilon(t)} = L_o * \{(\sigma_r + 1)\tilde{\imath}_r(t) e^{j\varepsilon(t)} + \tilde{\imath}_s(t)\} = L_o * \tilde{\imath}_{mr}(t) \ldots\ldots\ldots\ldots \text{(2.27)}$$

Therefore $\tilde{\imath}_{mr}(t)^s = \{(\sigma_r + 1)\tilde{\imath}_r(t) e^{j\varepsilon(t)} + \tilde{\imath}_s(t)\}$ ……..……..... (2.28)

$$\Rightarrow \tilde{\imath}_r(t) = [\tilde{\imath}_{mr}(t) - \tilde{\imath}_s(t)] e^{-j\varepsilon(t)} \{\frac{1}{(\sigma_r + 1}\} \ldots\ldots\ldots\ldots\ldots\ldots \text{(2.29)}$$

Putting this in (2.16),

$$R_r * [\,\tilde{\imath}_{mr}(t) - \tilde{\imath}_s(t)]e^{-j\varepsilon(t)}\{\frac{1}{(\sigma_r+1}\} + L_o\,[\,\tilde{\imath}_{mr}(t) - \tilde{\imath}_s(t)]e^{-j\varepsilon(t)} + L_o\,\frac{d(\,\tilde{\imath}_s(t)*e^{-j\varepsilon(t)}\,)}{dt} = 0$$

$$\Rightarrow R_r * [\,\tilde{\imath}_{mr}(t) - \tilde{\imath}_s(t)]e^{-j\varepsilon(t)}\{\frac{1}{(\sigma_r+1}\} + L_o\,\frac{d}{dt}[\,\tilde{\imath}_{mr}(t) - j\,\frac{d\varepsilon(t)}{dt}\,\tilde{\imath}_{mr}(t)\,L_o]e^{-j\varepsilon(t)} = 0 \;..\; (2.30)$$

The above resulting equation in stator coordinates will be ((2.30) * $e^{j\varepsilon(t)}$)

$$L_o\frac{d}{dt}\tilde{\imath}_{mr}(t) + \frac{R_r}{\sigma_r+1}\tilde{\imath}_{mr}(t) - jw_rL_o\tilde{\imath}_{mr}(t) - \frac{R_r}{\sigma_r+1}\tilde{\imath}_s(t) = 0$$

Where $w_r = \frac{d\varepsilon(t)}{dt}$ & $\tilde{\imath}_{mr}(t) = i_{mr}(t) * e^{j\rho(t)}$

Putting the value of $\tilde{\imath}_{mr}(t)$ in above equation

$$L_o\frac{d}{dt}i_{mr}(t) * e^{j\rho(t)} + \frac{R_r}{\sigma_r+1}i_{mr}(t) * e^{j\rho(t)} - jw_rL_oi_{mr}(t) * e^{j\rho(t)} - \frac{R_r}{\sigma_r+1}\tilde{\imath}_s(t) = 0$$

$$\Rightarrow [L_o\frac{d}{dt}i_{mr}(t) + jL_o\frac{d\rho}{dt}i_{mr}(t) + \frac{R_r}{\sigma_r+1}i_{mr}(t) - jw_rL_oi_{mr}(t)]\,e^{j\rho(t)} = \frac{R_r}{\sigma_r+1}\tilde{\imath}_s(t)$$

If the above equation is transformed into rotor flux coordinates by multiplying $e^{-j\rho(t)}$, giving

$$L_o\frac{d}{dt}i_{mr}(t) + \frac{R_r}{\sigma_r+1}i_{mr}(t) - j(w_{mr} - w_r)L_oi_{mr}(t) = \frac{R_r}{\sigma_r+1}\tilde{\imath}_s(t)e^{-j\rho(t)} \ldots\ldots\ldots\ldots\ldots (2.31)$$

Where $w_r = \frac{d\rho(t)}{dt}$ is the instantaneous angular speed of the rotor field flux.

If the co-ordinates of the stator current in this system are denoted by i_{ds}(t) and i_{qs}(t), then

$$\tilde{\imath}_s(t)e^{-j\rho(t)} = i_{ds}(t) + j i_{qs}(t)$$

Separating (2.31) into real and imaginary parts as follows:

$$L_o\frac{d}{dt}i_{mr}(t) + \frac{R_r}{\sigma_r+1}i_{mr}(t) = \frac{R_r}{\sigma_r+1}i_{sd}(t)$$

$$(w_{mr} - w_r)L_oi_{mr}(t) = \frac{R_r}{\sigma_r+1}i_{sq}(t)$$

Since $\frac{L_o(\sigma_r+1)}{R_r} = \frac{L_r}{R_r} = T_r = \text{rotor time constant}$

The above equations can be written as

$$T_r\frac{d}{dt}i_{mr}(t) + i_{mr}(t) = i_{sd}(t) \ldots\ldots\ldots\ldots\ldots\ldots\ldots\ldots\ldots\ldots\ldots\ldots\ldots\ldots\ldots\ldots\ldots\ldots\ldots\ldots\ldots\ldots (2.32)$$

$$(w_{mr} - w_r) = \frac{1}{T_r * i_{mr}(t)} i_{sq}(t) \quad \text{..... (2.33)}$$

2.4.3. Torque Equation

From (2.17), electromagnetic torque is

$$M_d = \frac{2}{3}\frac{P}{2} M\, I_m[\, \tilde{\imath}_s(t) \left\{\tilde{\imath}_r(t)\, e^{j\varepsilon(t)}\right\}^* \,]$$

$$= \tfrac{2}{3}\tfrac{P}{2}\tfrac{L_0}{1+\sigma_r}\, I_m[\, \tilde{\imath}_s(t) \{\, \tilde{\imath}_{mr}(t)^s - \tilde{\imath}_s(t)\} \,\}^*] \text{(From (2.28)}$$

$$= \tfrac{2}{3}\tfrac{P}{2}\tfrac{L_0}{1+\sigma_r}\, I_m[\, \tilde{\imath}_s(t) \{\, \tilde{\imath}_{mr}(t)^s\}^*]$$

$$= \frac{2}{3}\frac{P}{2}\frac{L_0}{1+\sigma_r}\, I_m[\, \tilde{\imath}_s(t) \left\{\, i_{mr}(t) * \, e^{j\rho(t)}\right\}^* \,]$$

$$= \frac{2}{3}\frac{P}{2}\frac{L_0}{1+\sigma_r}\, I_m[\, i_{mr}(t)\left\{\, \tilde{\imath}_s(t) \, * \, e^{-j\rho(t)}\right\}]$$

$$= \frac{2}{3}\frac{P}{2}\frac{L_0}{1+\sigma_r}\, I_m[\, i_{mr}(t)\left\{\, i_{ds}(t) + j i_{qs}(t)\right\}]$$

$$= \tfrac{2}{3}\tfrac{P}{2}\tfrac{L_0}{1+\sigma_r}\, [\, i_{mr}(t) * \left\{i_{qs}(t)\right\}] \quad \text{..... (2.34)}$$

CHAPTER 3

FIELD ORIENTED CONTROL (VECTOR CONTROL)

3.1. BASIC CONCEPT

The scalar control techniques like V/f control of inverter-fed induction motor gives good steady state but poor dynamic response. The poor dynamic performance is due to the deviation of the air gap flux linkages from their set values while changing the speed reference. The oscillations in the air gap flux linkages result in oscillation in electromagnetic torque which leads to speed oscillations making the system highly unreliable.

Separately excited dc motor drives provides very simple control because of independent flux circuit. By keeping the flux constant, we can change the armature current to have an independent control of torque. This is possible because of two separate windings present in separately excited DC- Machine i.e. armature and field winding. Moreover, the dc motor control requires only the control of magnitudes of field or armature current, whereas in ac machine we have to control both magnitude and phase.

The induction motor drive has complex control strategy because it requires a coordinated control of stator current magnitudes, frequencies and their phases. So to have a DC motor like control we need to have two independent circuits for torque and flux i.e. torque and flux components need to be orthogonal. So to have a separately excited DC motor like control, stator current phasor can be resolved into two orthogonal components i.e. one component along the rotor flux linkages, which is the field-producing current and other component is perpendicular to it which will be controlled for torque.

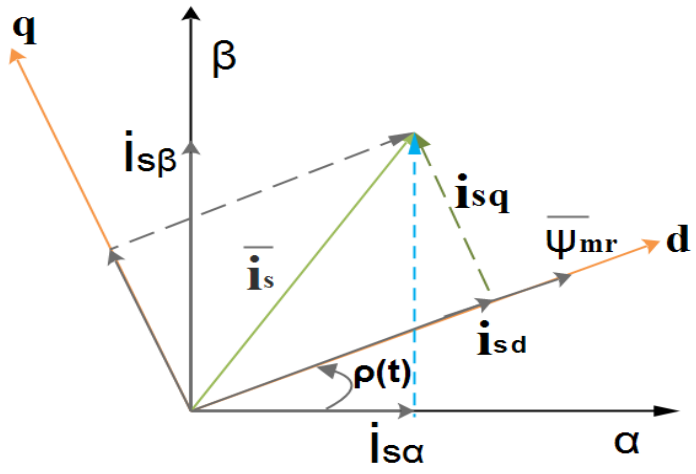

Fig 3.1: Stator Current Space Vector & Its Component along d-q & α-β reference frame

In Fig-2.4, if ψ_{mr} (rotor field flux) is aligned along the d-axis (which is rotating at synchronous speed) as in Fig-3.1, all the space phasors will appear as dc quantities if looked from d-q reference frame. d-q components can be calculated from α-β components & rotor field flux position, ρ(t). If we can calculate correct rotor flux position at every instant, d-q components can be easily determined. So it is called "*Field Oriented Control"* or "*Vector control*" as it relates to the space phasor control of the rotor field flux linkages.

3.2. TYPES OF VECTOR CONTROL

There is basically two major categories of vector control, direct and indirect or feed forward method, invented by Blaschke and Hasse respectively. Both methods are different by how they generate the unit vector i.e. cos ρ(t) & sine ρ(t).

3.2.1. Direct vector control:

Here air gap flux of the machine is directly measured by measuring the induced voltage in hall-sensors or flux sensing coils and integrating it. However, there are several difficulties in this approach.

- The motor has to be specially designed to accommodate the sensing device.
- Hall-sensors are fragile in nature, so extra care has to be taken.
- At low frequencies, voltage signal V_{ds} & V_{qs} are very low. In addition, ideal integration becomes difficult because of the dc offset, which limits the lowest speed at which the technique can be used.
- The induced voltage in the sensing devices contain harmonics due to rotor slots which is difficult to filter as their frequencies changes with the speed of the machine.

The primary advantage in this method is immunity from parameter variation. Because the measurements are independent of machine parameters values like resistance and inductances, which changes with temperature, saturation etc.

In some cases instead of using voltages from sensing coils, the machine terminal voltage can be used, but in this case, the stator resistance drop has to be compensated before integration. Since resistance changes with temperature, this method is also difficult to implement especially during low speed operations.

3.2.2. Indirect vector control

This method estimates the model equations of the machine with easily measurable quantities as inputs and calculates the magnitude and position of the rotor flux.

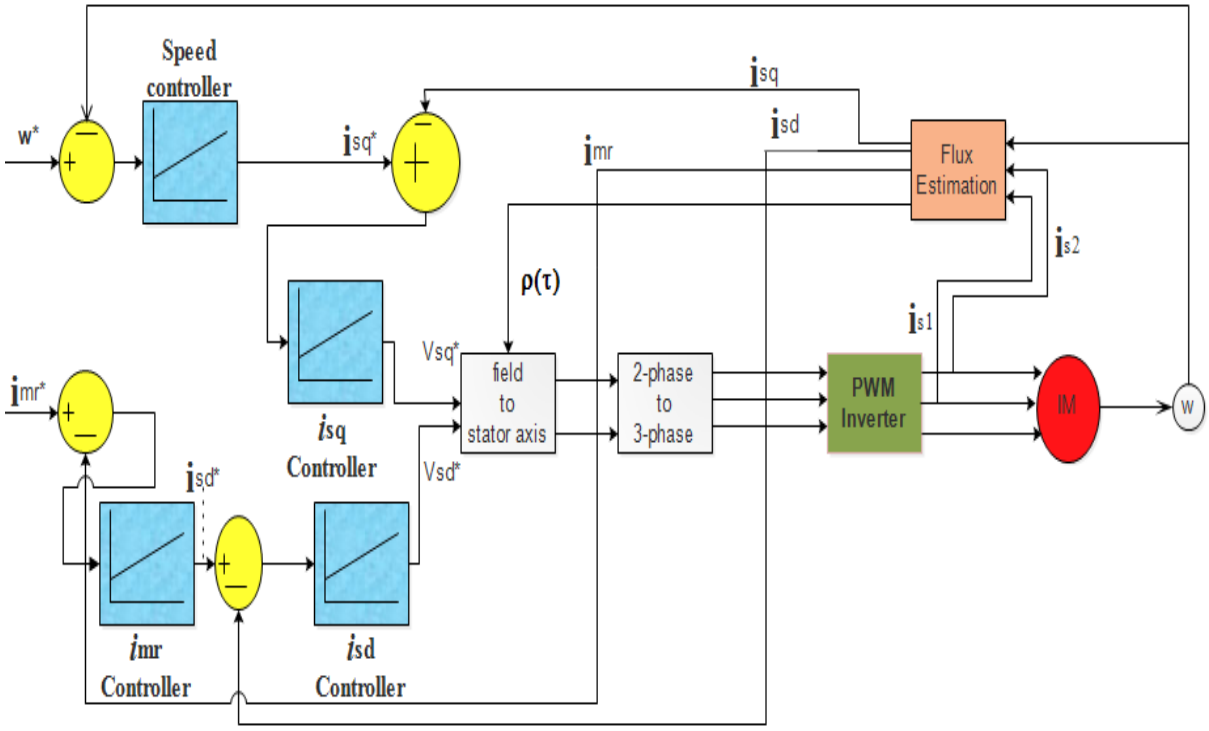

Fig 3.2: Block diagram of Indirect Vector Control

Fig-3.2 shows how it can be used to generate information regarding the actual values of i_{qs}, $i_{ds,}$ i_{mr} , torque M_d and the angle ρ (t) that rotor flux makes with the stator axis.

Decoupling in indirect vector control is very precise compared to direct vector control due to feed-forward technique. To change the flux, the input $i_{ds}(t)$ should be changed & to change the torque the input $i_{qs}(t)$ is to be changed, without disturbing $i_{mr}(t)$ by changing $i_{ds}(t)$. The response of $i_{mr}(t)$ is slow compared to $i_{qs}(t)$ because the large rotor time constantT_r. The torque response is fast & instantaneous as it does not have any limiting time constants under this type of control.

3.3. TRANSFORMATION RELATIONSHIP

From Fig-3.1 various conversion relationships can be done such as:

- α-β to d-q transformation: ……...……...…. (3.1)

$$i_{ds}(t) = i_{s\alpha}(t)\ cos\rho(t) + \ i_{s\beta}(t)\ sin\rho(t)$$

$$i_{qs}(t) = i_{s\beta}(t)\ cos\rho(t) - \ i_{s\alpha}(t)\ sin\rho(t)$$

- d-q to α-β transformation: ……..….(3.2)

$$i_{s\alpha}(t) = i_{ds}(t)\ cos\rho(t) - \ i_{qs}(t)\ sin\rho(t)$$

$$i_{s\beta}(t) = i_{qs}(t)\ cos\rho(t) + \ i_{ds}(t)\ sin\rho(t)$$

- 2-phase to 3-phase transformation: ……..….. (3.3)

$$i_{s1}(t) = \frac{2}{3}\ i_{s\alpha}(t)$$

$$i_{s2}(t) = \frac{-1}{3}\ i_{s\alpha}(t) + \frac{1}{\sqrt{3}}\ i_{s\beta}(t)$$

$$i_{s3}(t) = \frac{-1}{3}\ i_{s\alpha}(t) - \frac{1}{\sqrt{3}}\ i_{s\beta}(t)$$

- 3-phase to 2-phase transformation: ……..… (3.4)

$$i_{s\alpha}(t) = \frac{3}{2} i_{s1}(t)$$

$$i_{s\beta}(t) = \frac{\sqrt{3}}{2}\ \{\ i_{s2}(t) - i_{s3}(t)$$

CHAPTER 4

INDUCTION MACHINE MODEL & SIMULATION RESULTS

4.1. INDUCTION MACHINE MODEL

The parameters of the induction motor used in the present work are given in table 4.1.

Table 4.1: Machines parameters used for Simulink

Machine Parameters used for simulation	
Three Phase wye-connected squirrel cage induction motor	
poles, P	4
Speed,N	1420 RPM
frequency,f	50 Hz
Voltage,V	415 volt
Power, W	1100 Watt
R_s	7.587 Ω
L_{ls}	0.022913 H
R_r	7.4719 Ω
L_{lr}	0.022913 H
L_m	0.580065 H
J	0.010622
B	0.001

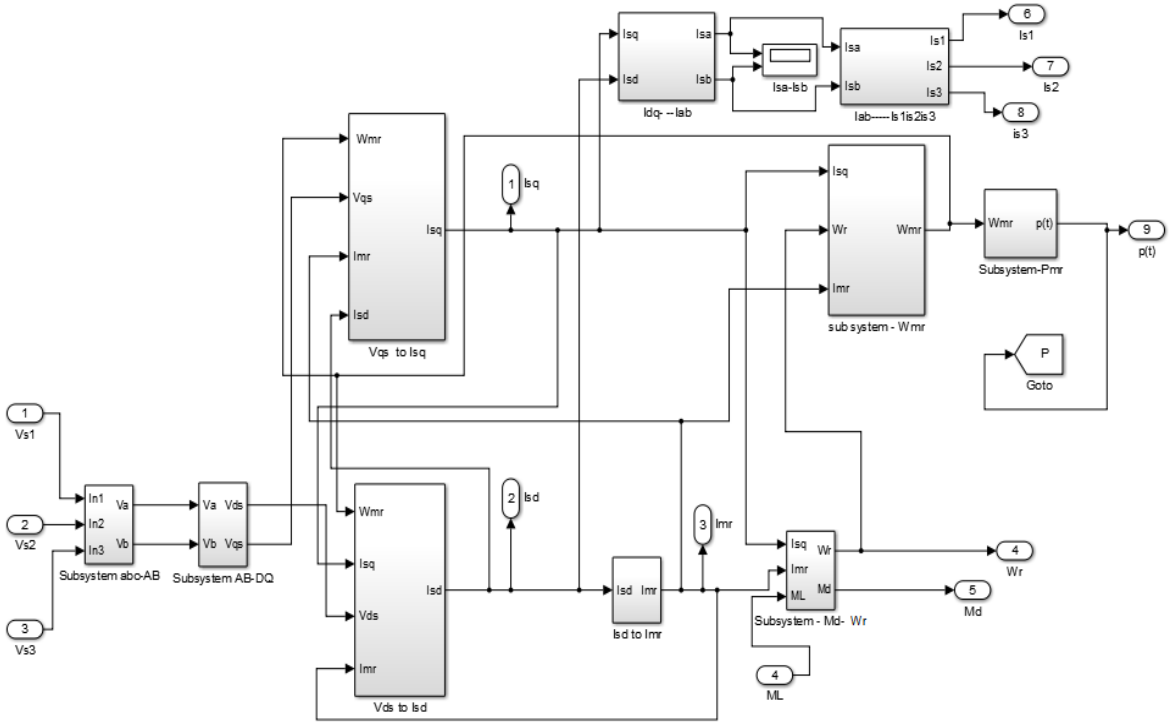

Fig 4.1: Induction motor model in Simulink

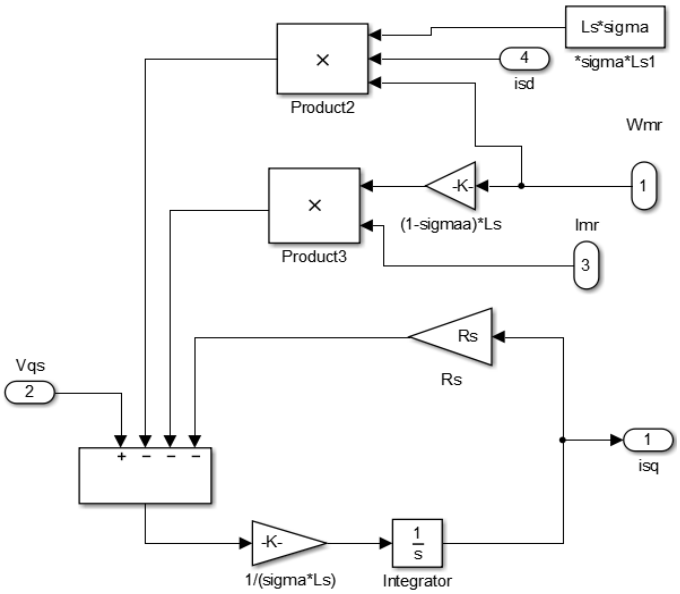

Fig 4.2: Subsystem v_{qs} to i_{qs}

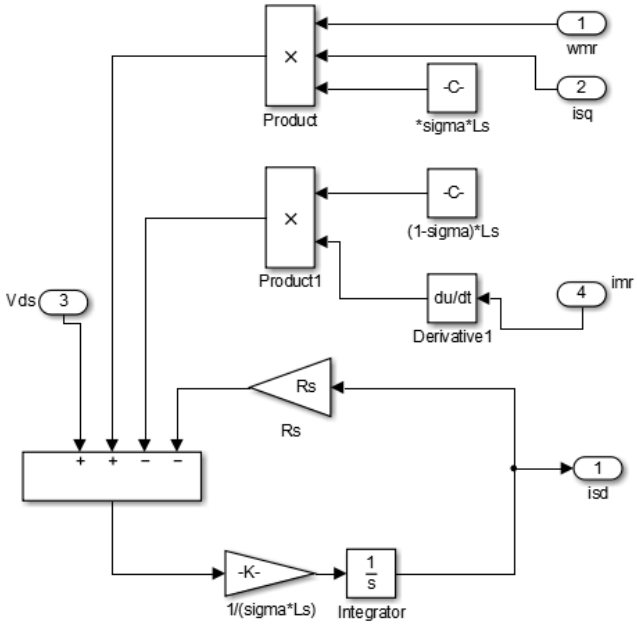

Fig 4.3: Subsystem v_{ds} to i_{ds}

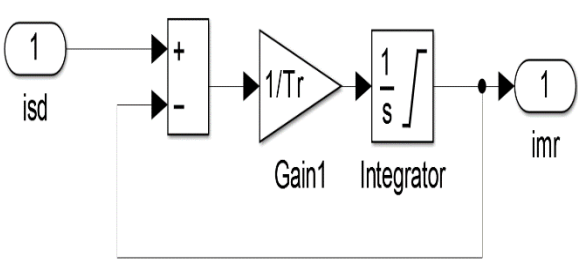

Fig 4.4: Subsystem i_{sd} to i_{mr}

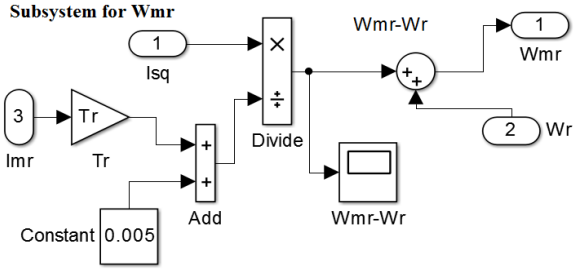

Fig 4.5: Subsystem i_{mr} to w_{mr}

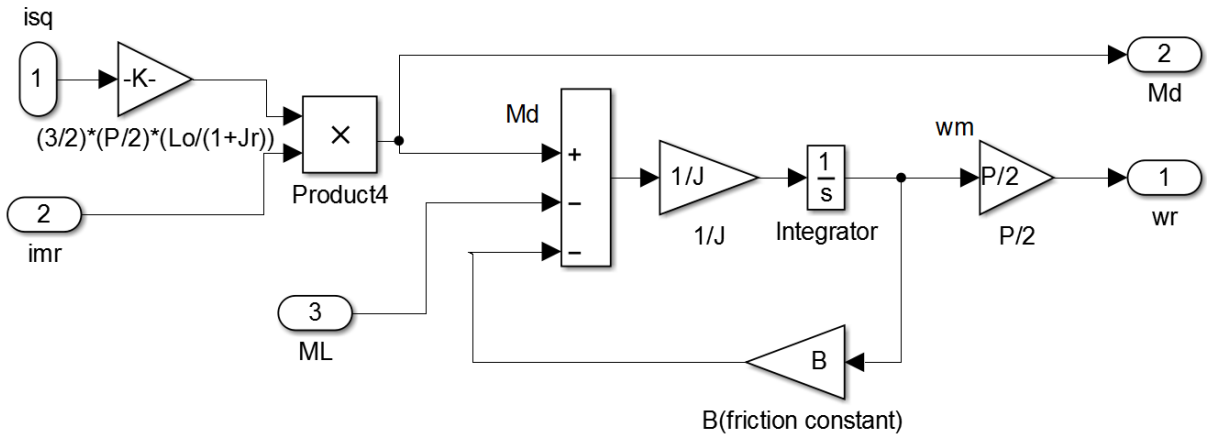

Fig 4.6: Subsystem for M_d & w_r

4.2. SIMULATION RESULTS & ANALYSIS:

The machine parameters in Table-4.1 were used to simulate the machine model. Three phase voltages of line voltage 415 volts was applied, load torque (M_l) was taken as zero. Various plots are analyzed as follows:

(i) $i_{s1} - i_{s2} - i_{s3}$ (Stator currents) plot:

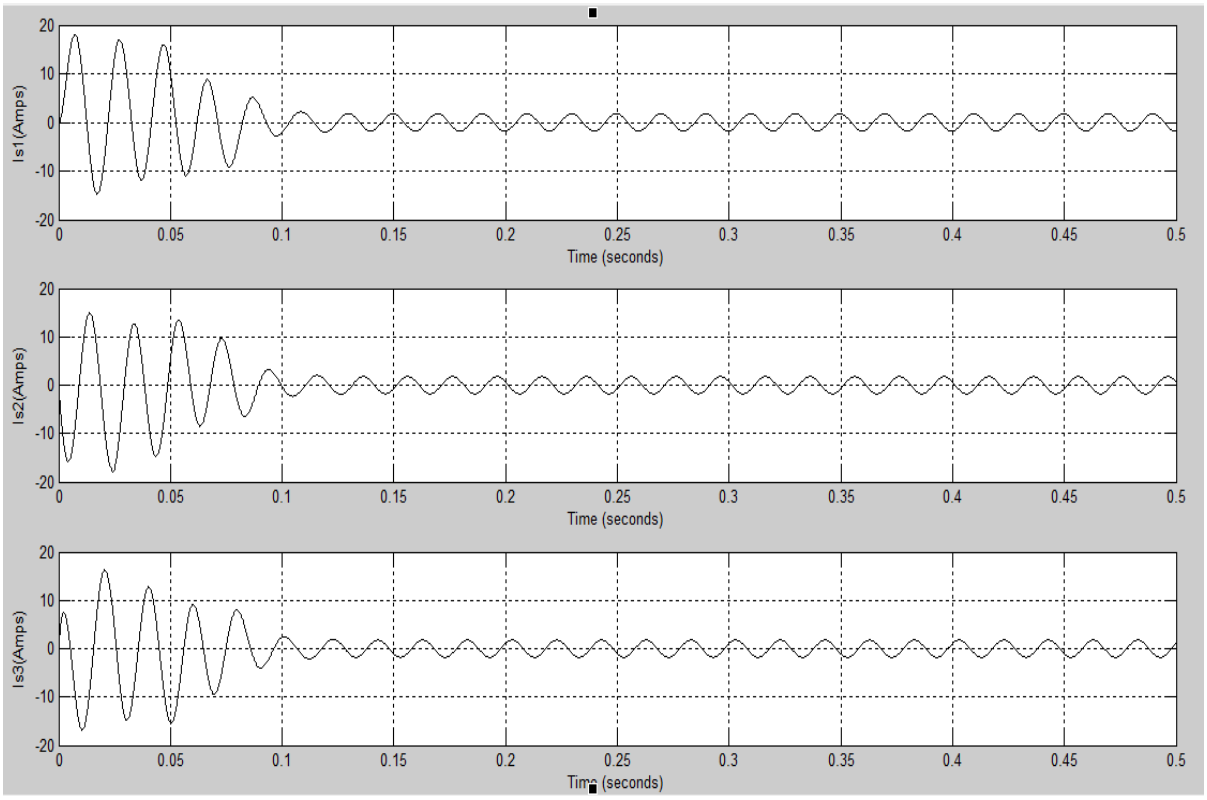

Fig 4.7: Induction motor model-Output stator currents

Fig No-4.7 shows the stator output currents which are sinusoidal and 120-degree phase displaced. It takes almost 0.1 sec to reach steady state. 0 to 0.1 sec shows the transient response of all three phase currents.

(ii) Speed Response (w_{mr}):

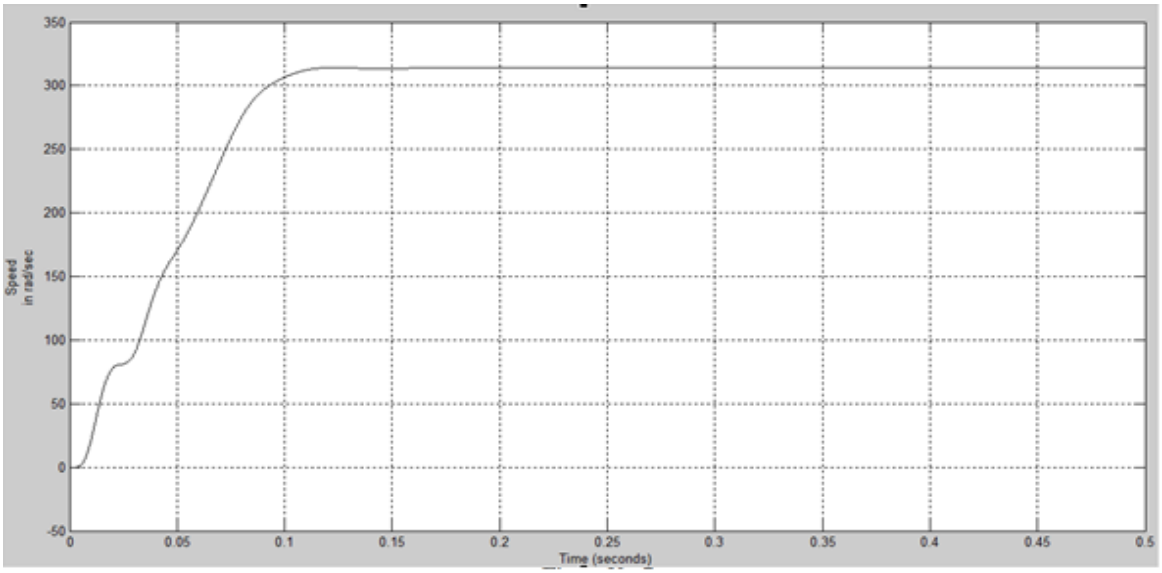

Fig 4.8: Induction motor model- Electrical Speed response

Fig-4.8 shows the speed response of the induction motor which settles at 314 rad/sec which is the electrical speed of the motor for 50 H_z frequency.

(iii) Electromagnetic Torque Response (M_d):

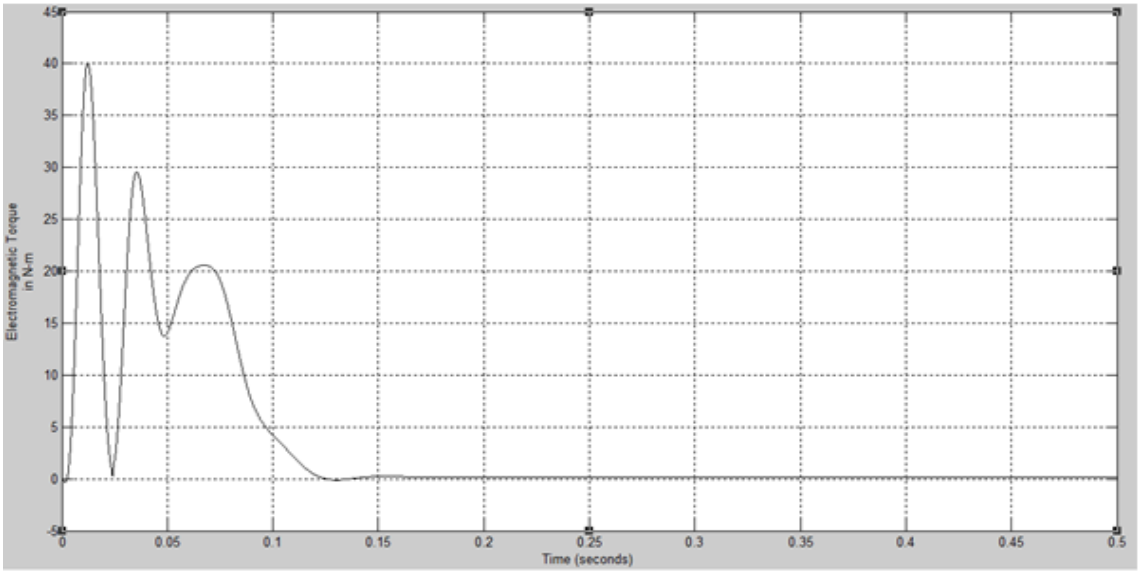

Fig 4.9: Induction motor model-Electromagnetic torque response

Fig-4.9 shows the torque response of the machine. Torque is in transient state as long as speed has not attained the steady state, once the speed reaches 314 rad/sec, torque comes down to 0.

(iv) $i_{sq} - i_{sd}$ plot:

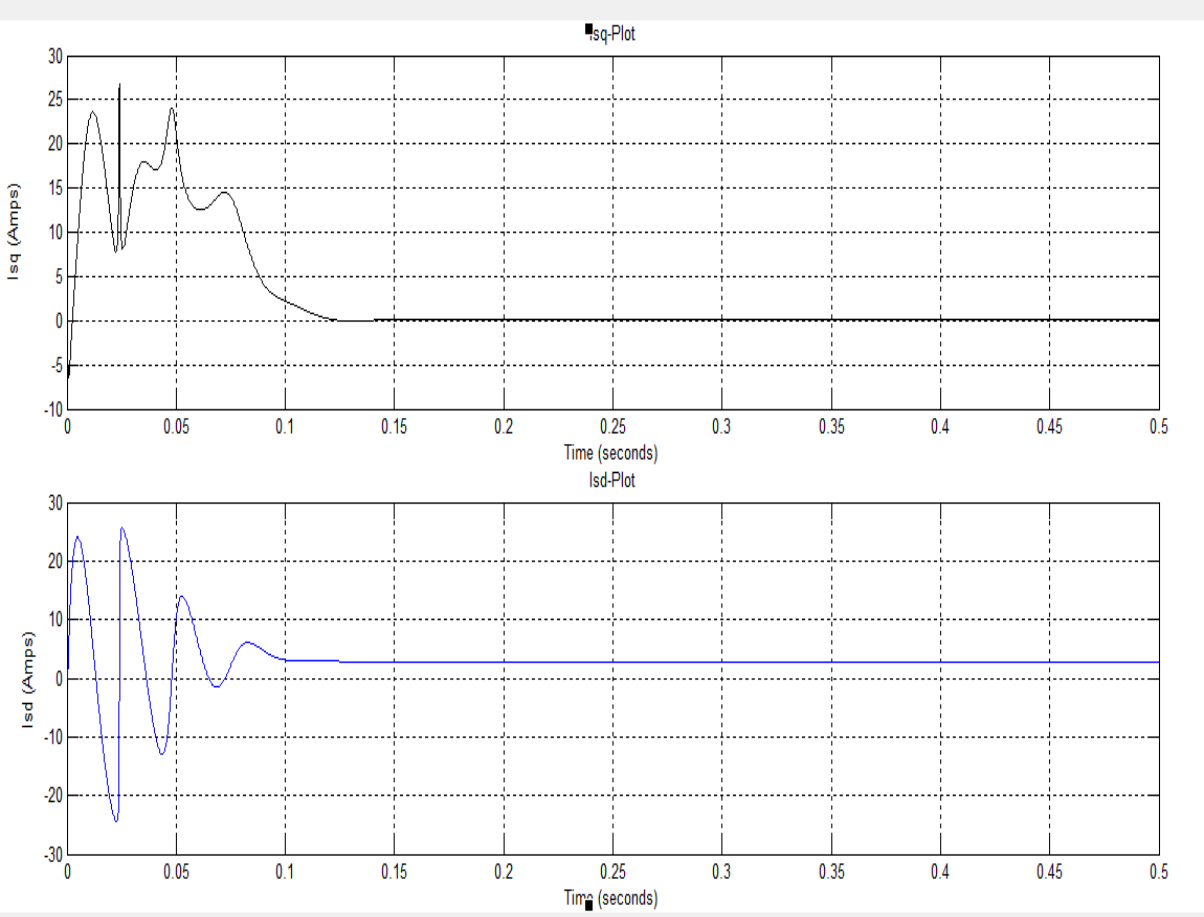

Fig 4.10: Induction motor model- $i_{sq} - i_{sd}$ currents' response

Fig-4.10 shows $i_{sq} - i_{sd}$ response respectively. i_{sq} response is almost same as torque, i.e. when i_{sq} also comes to zero, torque comes down to '0'.

On the other hand i_{sd} is constant at 2.68 Amps & appears as DC quantity as desired, because it is aligned along rotor flux axis & rotating with synchronous speed. It represents flux of the machine where as i_{mr} is instantaneous value of i_{mr}. Under steady state both i_{mr} & i_{sd} has same value.

CHAPTER 5

INDIRECT VECTOR CONTROL MODEL & RESULTS

5.1 VECTOR CONTROL MODEL:

Fig-5.1 shows the implementation of vector control technique. Speed and flux reference is fed to the speed-controller and i_{mr}- controllers respectively. The output of the speed controller is fed to i_{sq} – controller & output of i_{mr} –controller was fed to i_{sd}– controller. The output of i_{sq} & i_{sd} – controller is considered as $v_{sq}*$ & $v_{sd}*$ reference respectively.

Then v_{sq} & v_{sd} are converted to stationary reference $v_{s\beta}$ & $v_{s\alpha}$ voltages which after converted to 3-phase voltage, are fed to a sine PWM modulator, then to a VSI having DC-link voltage 650 volts. The output of the inverter is fed to the machine model.

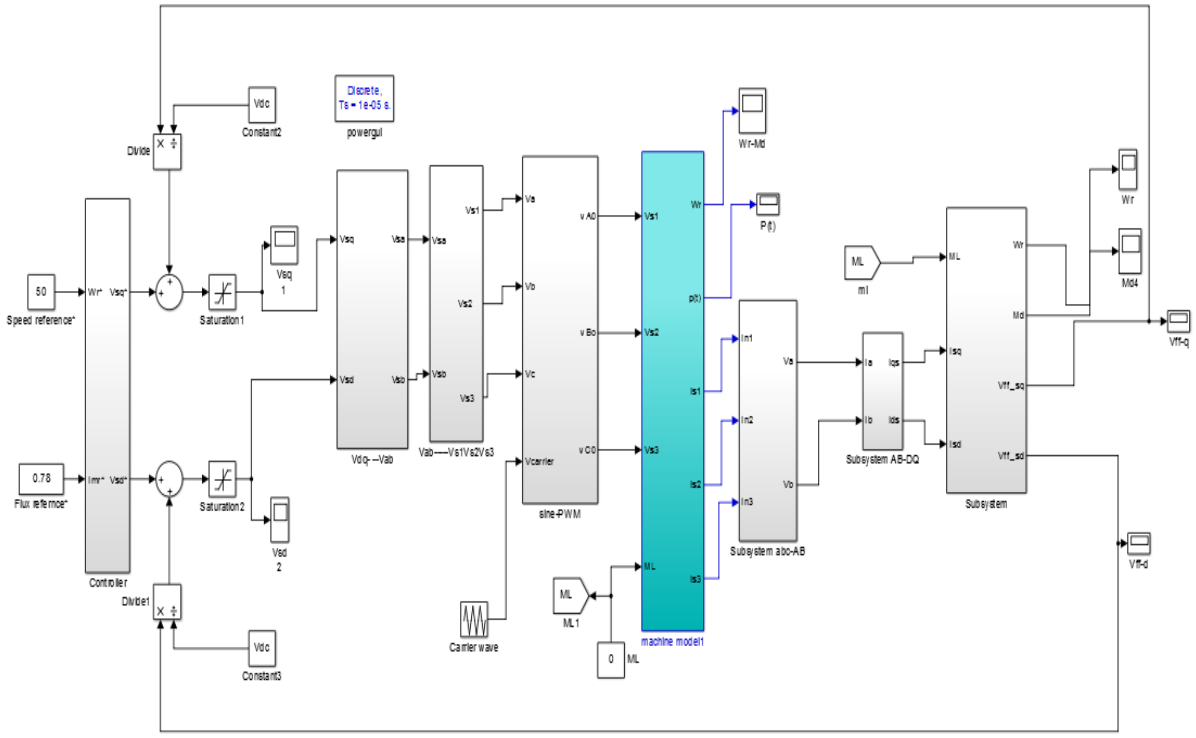

Fig 5.1: Simulink model for vector control

5.2. CONTROLLER DESIGN: (PI-CONTROLLERS)

Four PI-controllers are used for i_{sq}, i_{sd}, i_{mr} & w_r control. i_{sq} corresponds to torque control whereas i_{mr} & i_{sd} corresponds to flux-response, w_r corresponds to speed-controller. The design of various controllers are discussed below.

i_{qs}^{*} - controller design:

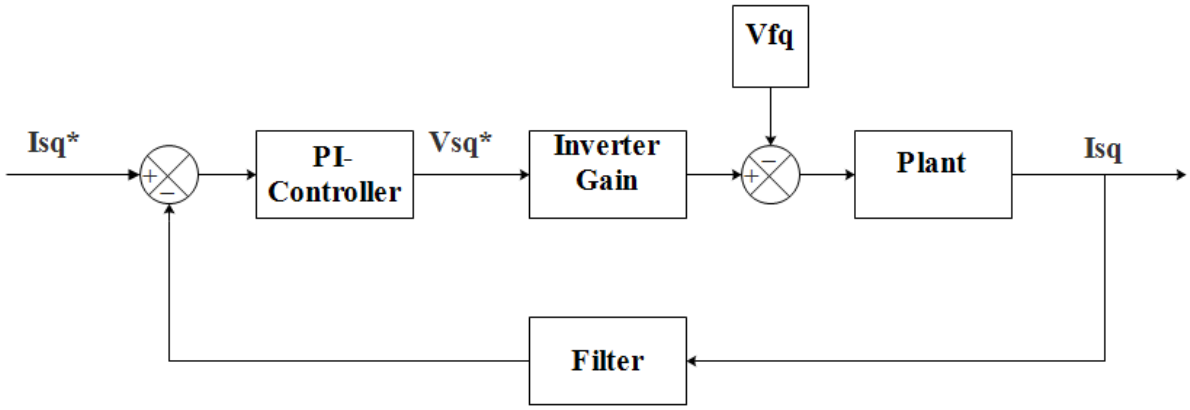

Fig 5.2: i_{sq} (torque) controller

From (2.26)

$$v_{qs}= R_s\, i_{qs} + \sigma\, L_s i_{ds} w_{mr} + \sigma\, L_s \frac{di_{qs}}{dt} + (1-\sigma)\, L_s i_{mr} w_{mr}$$

$$\Rightarrow v_{qs}= \{R_s\, i_{qs} + \sigma\, L_s \frac{di_{qs}}{dt}\} + \{\sigma\, L_s i_{ds} w_{mr} + (1-\sigma) L_s i_{mr} w_{mr}\}$$

Taking Laplace transform of the above equation:

$$v_{qs}(s)= \{\, R_s\, i_{qs}(s) + \sigma\, s L_s i_{qs}(s)\} + v_{fq} \ldots\ldots\ldots\ldots\ldots\ldots \text{(5.1)}$$

Where $v_{fq} = \sigma\, L_s i_{ds} w_{mr} + (1-\sigma)\, L_s i_{mr} w_{mr}$= constant

So from (5.1),

$$i_{qs}(s)= \frac{v_{qs}(s) - v_{fd}}{(\, R_s + \sigma\, s L_s)} \ldots\ldots\ldots\ldots\ldots\ldots\ldots\ldots\ldots\ldots\ldots\ldots \text{(5.2)}$$

$$i_{qs}(s)= \frac{v_{qs}(s) - v_{fd}}{R_s(1+\frac{\sigma\, s L_s}{R_s})} = \frac{\{v_{qs}(s) - v_{fd}\} * (1/R_s)}{(1+sT_{qs})} \ldots\ldots\ldots\ldots\ldots\ldots \text{(5.3)}$$

Where $T_{qs} = \frac{\sigma\, L_s}{R_s}$ …….. (5.4)

So open gain loop will be $K_{isq}\left(\frac{1+sT_{isq}}{sT_{isq}}\right) * V_{dc} * (\frac{\frac{1}{R_s}}{1+sT_{qs}}) = \frac{1}{sT_b}$ …….. (5.5)

Where V_{dc} = inverter gain

T_b= PI-controller's bandwidth

By making$T_{qs} = T_{isq}$, (5.5) will be

$$K_{isq} = \frac{R_s * T_{isq}}{T_b * V_{dc}} \quad \text{..... (5.6)}$$

$$K_{iisq} = \frac{K_{isq}}{T_{isq}} \quad \text{..... (5.7)}$$

i_{ds}^* - controller design

$$K_{isd} = K_{isq} \quad \text{..... (5.8)}$$

$$K_{iisd} = K_{iisq} \quad \text{..... (5.9)}$$

Where $v_{fd} = (1\text{-}\sigma)\, L_s \frac{di_{mr}}{dt} - \sigma\, L_s i_{qs} w_{mr}$= constant ..... (5.10)

w_r^* - controller design (speed controller)

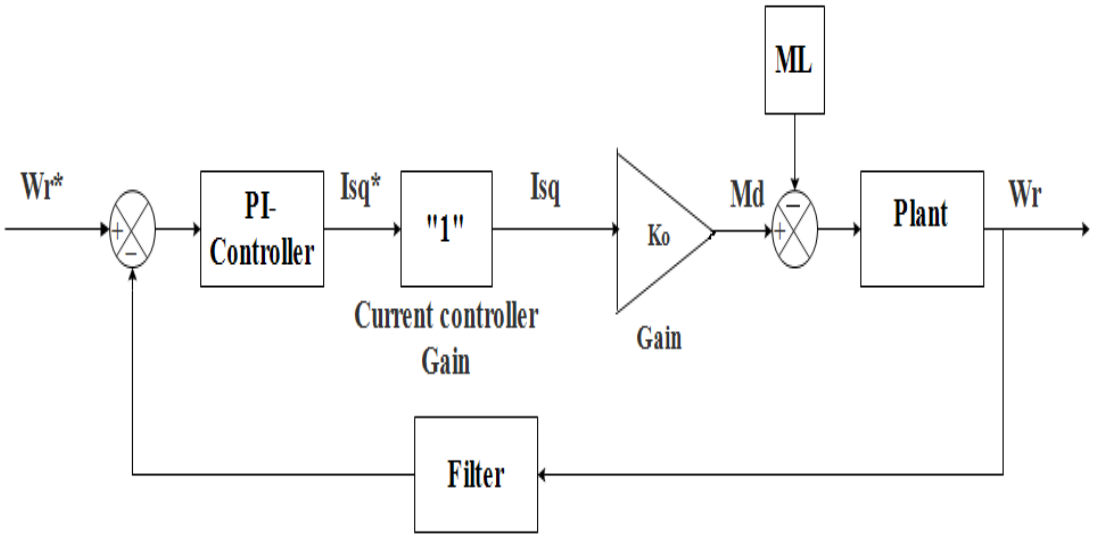

Fig 5.3: w_r (Speed) controller

From (2.18)

$$J \frac{dw_m}{dt} + B w_m = M_d - M_l$$

$$\Rightarrow w_m = \frac{M_d - M_l}{Js + B} \quad \text{..... (5.11)}$$

$$\& \ w_r = (w_m * \frac{P}{2}) \ \ldots\ldots\ldots\ldots\ldots\ldots\ldots\ldots\ldots\ldots\ldots \ (5.12)$$

So open gain loop will be $K_w \left(\frac{1+sT_w}{sT_w}\right) * K_o * \left(\frac{\frac{1}{B}}{1+s(J/B)}\right)$

By taking $T_w = J/_B$ …………………………………….… (5.13)

& considering $K_w \left(\frac{1+sT_w}{sT_w}\right) * K_o * \left(\frac{\frac{1}{B}}{1+s(J/B)}\right) = \frac{1}{sT_b}$

$$\Rightarrow K_w = \frac{B * T_w}{K_o * T_b} \ldots\ldots\ldots\ldots (5.14)$$

$$\text{So } K_{iw} = \frac{K_w}{T_w} \ldots\ldots\ldots\ldots (5.15)$$

$$\text{Where } K_o = \frac{2}{3}\frac{P}{2}\frac{L_O}{1+\sigma_r} i_{mr} \ldots\ldots\ldots\ldots (5.16)$$

$i_{mr}{}^*$ - controller design:

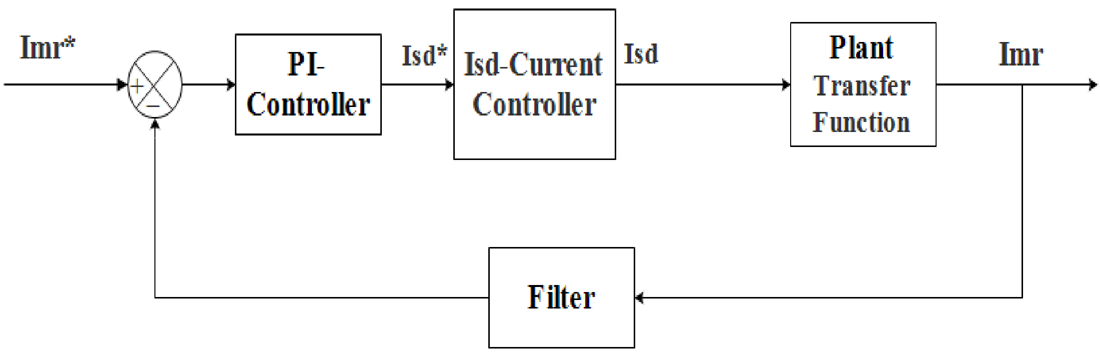

Fig 5.4: i_{mr}- controller

From (2.32)

$$T_r \frac{d}{dt} i_{mr}(t) + i_{mr}(t) = i_{sd}(t)$$

Taking Laplace transformation:

$$\Rightarrow i_{mr}(s) = \frac{i_{sd}(s)}{(1+sT_r)} \ldots\ldots\ldots\ldots (5.17)$$

So open loop gain will be

$$K_{imr}\left(\frac{1+sT_{imr}}{sT_{imr}}\right) * \left(\frac{1}{1+sT_r}\right) = \frac{1}{sT_b}$$

Taking $T_{imr} = T_r$ ..... (5.18)

$$\Rightarrow K_{imr} = \frac{T_{imr}}{T_b} \text{..... (5.19)}$$

$$K_{iimr} = \frac{K_{imr}}{T_{imr}} \text{ ..... (5.20)}$$

5.3. SINE PWM TECHNIQUE (SPWM)

Fig 5.5 shows a reference sine-wave is compared with a high frequency carrier wave. When the magnitude of sine wave is greater than the carrier wave magnitude, output remains at 1 & when the magnitude of sine wave drops below carrier wave, the output shifts to 0.

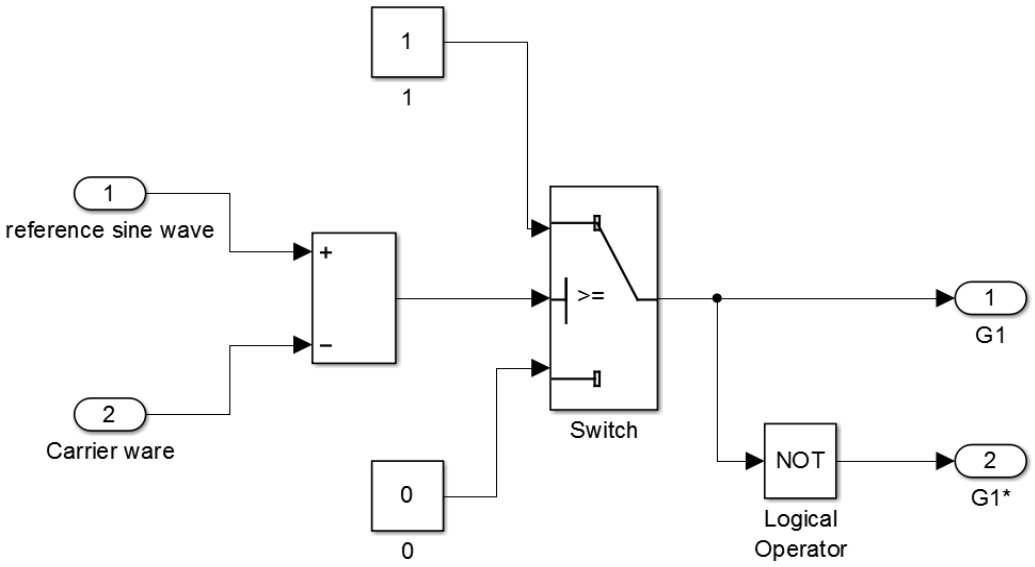

Fig 5.5: Simulink model for SPWM- Technique

Fig 5.6 shows the Simulink model for a 2-level inverter with SPWM firing technique. Here all the top switches are controlled whereas the bottom switches are complement of top switches.

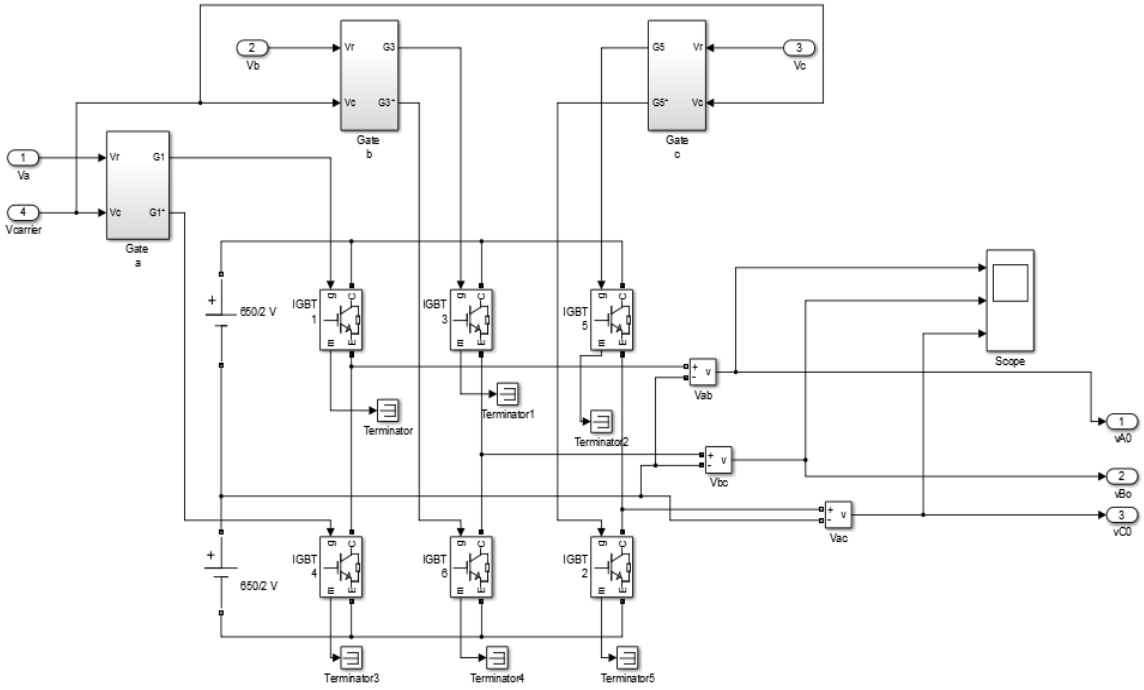

Fig 5.6: Simulink model for Sine-PWM

5.4. SIMULATION RESULTS FOR VECTOR CONTROL & ANALYSIS:

Expected Results:

The torque response should be fast & instantaneous whereas speed response should be comparatively slower than the torque response. Flux of the machine should always stay constant regardless of speed variation, torque disturbance etc. The torque response should follow i_{sq} where flux response should follow i_{sd}, as designed.

Initially the load torque will be kept zero. After some time when some positive load torque is applied to the motor, the speed drops down. To pull the speed back to original speed extra current i_{sq} will be supplied by the controller without disturbing i_{sd}.

Actual simulation results:

(1) Fig 5.7 shows the speed & torque variation for a given speed reference. Initially a speed reference of 100 rad/sec was applied to the vector control model. So the speed increases slowly from 0 to 100 rad/sec & torque increase from 0 to the maximum value i.e. 7 N-m. When the speed reaches the steady state, the torque comes down to 0 & follow a constant pattern. Same thing happens if we give a negative speed reference.

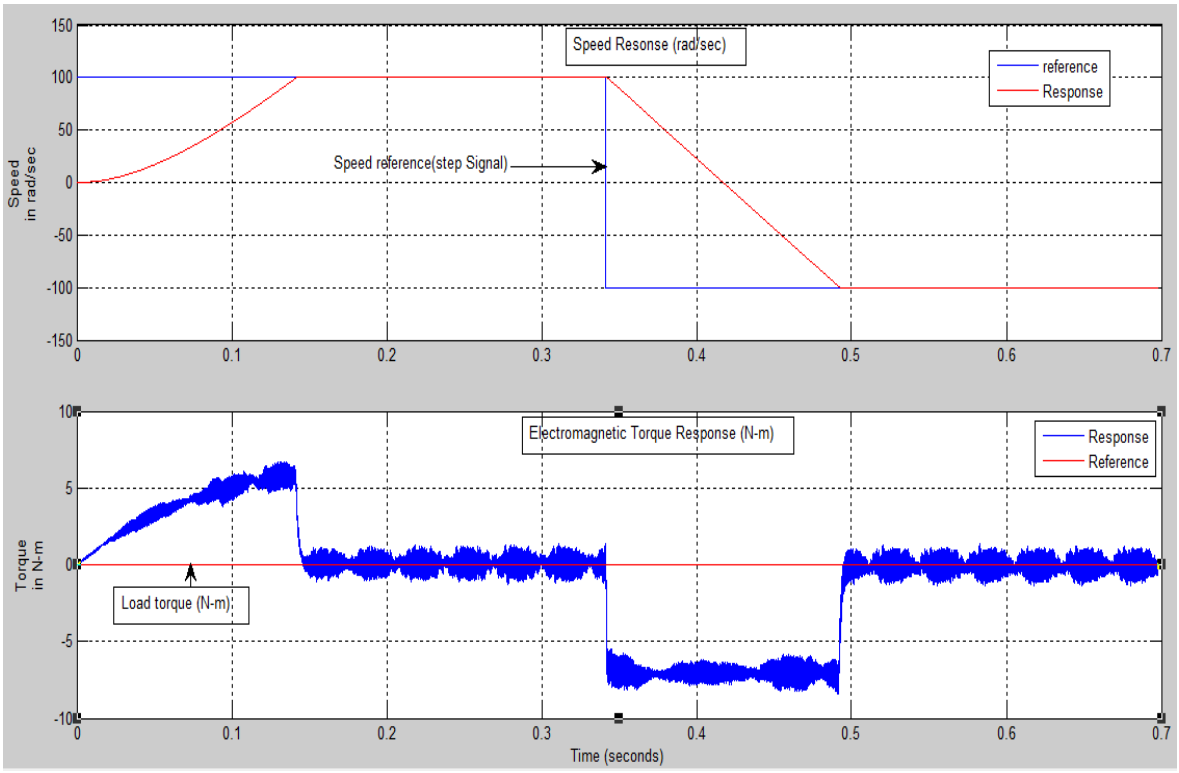

Fig 5.7: speed & torque response with speed reference variation

(2) Fig 5.8 shows speed & current response with different speed reference. We can clearly see a current reversal when there is a negative speed reference.

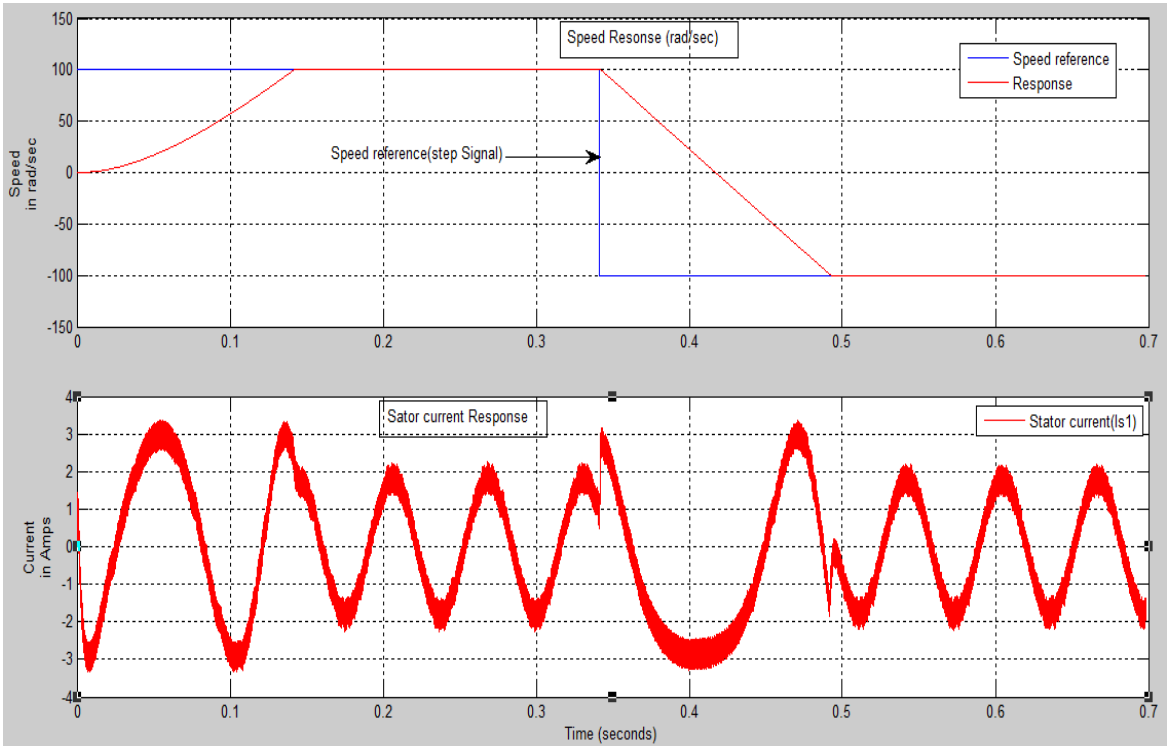

Fig 5.8: speed & current response with speed reference variation

(3) Fig 5.9 shows torque & Speed variation w.r.t load demand. As we can see from Fig-5.9, the speed remains almost constant irrespective of load variation.

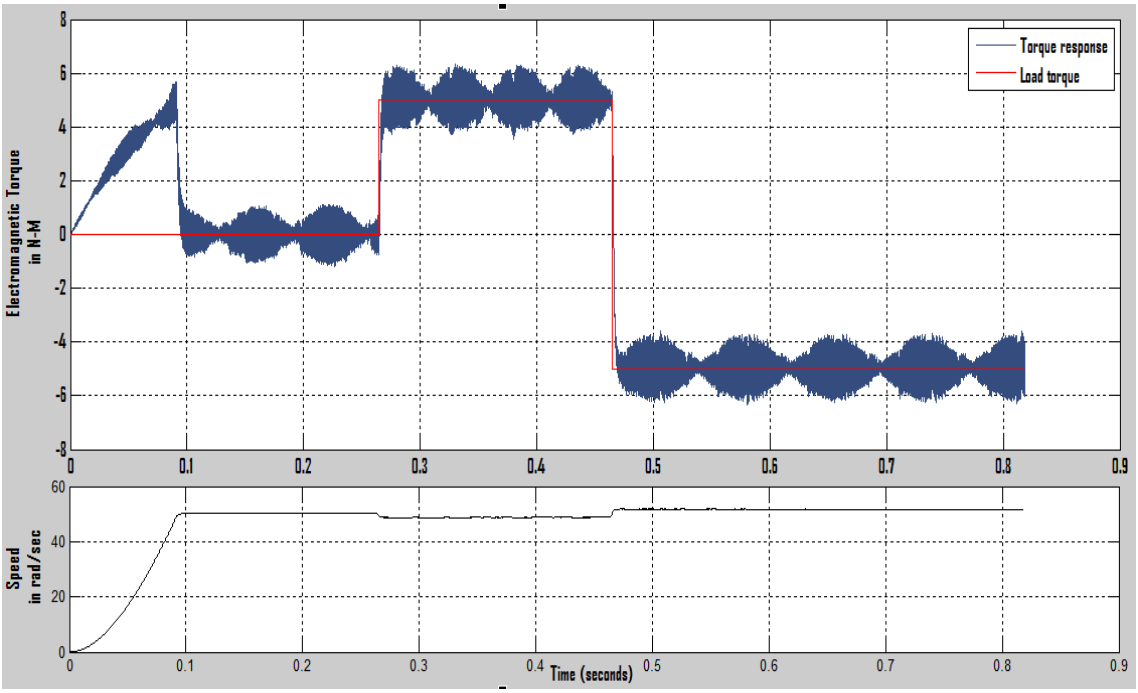

Fig 5.9: torque & speed response with load disturbance

(4) Fig 5.10 shows speed & torque variation corresponding to different speed & load reference.

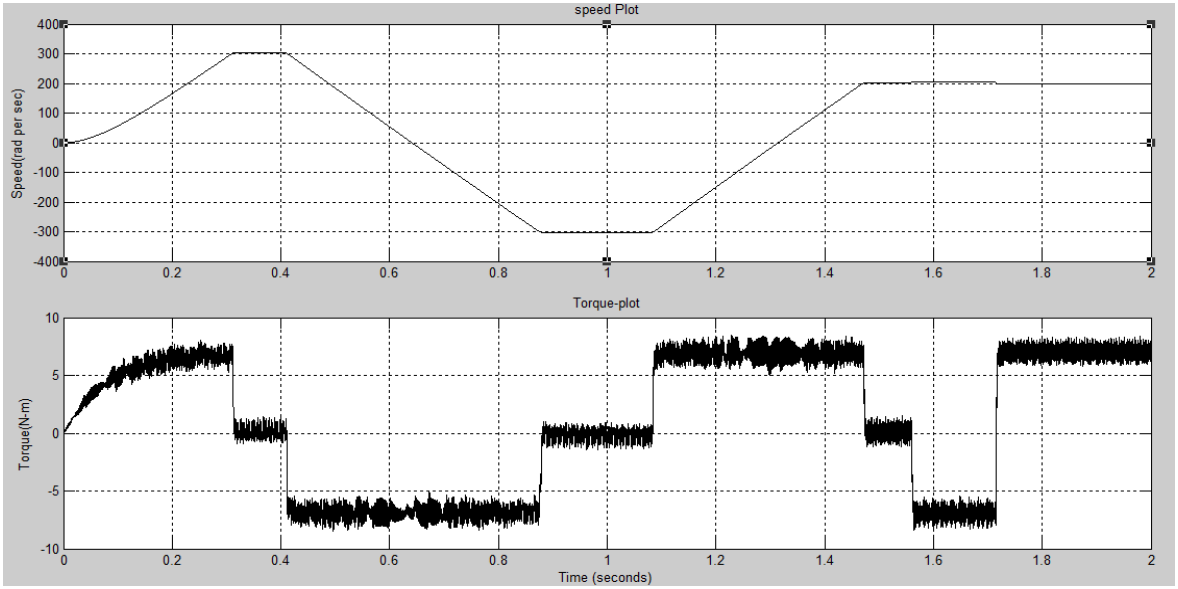

Fig 5.10: speed & torque response with speed & load disturbance

At starting, zero load-torque was given to the Simulink model. The starting speed reference was 300 rad/sec whereas starting $i_{mr}*$ reference was 2.678 Amps. Approximately after 0.3

sec speed reached the desired reference speed i.e. 300 rad/sec, during this time torque reached at maximum torque limit i.e. 7 N-m and stays there. Once the speed reached the steady state the torque comes down to zero. Thus the starting response is smooth.

Nearly at 0.42 sec speed reference was reversed to -300 rad/sec. Once the speed reversal signal was given, torque dropped down to negative peak i.e. – 7 N-m & stayed at this value as long as speed reached the desired reference speed i.e. -300 rad/sec. The moment speed reached the reference speed, the torque came back to zero again at approx. 0.87 sec. At approx. 1.1 sec speed reference was changed to 200 rad/sec, at that very instant torque went up to the positive peak i.e. +7 N-m & once the speed reached reference speed at 1.46 sec, torque came down to zero again.

At 1.55 sec load torque was changed from 0 to -7 N-m. The moment load torque was changed, torque came down to -7 N-m. At 1.67 sec while the speed remained same. When load torque changed to +7 N-m, torque is again increased to +7 N-m instantaneously. Thus the torque response is fast & instantaneous.

(5)

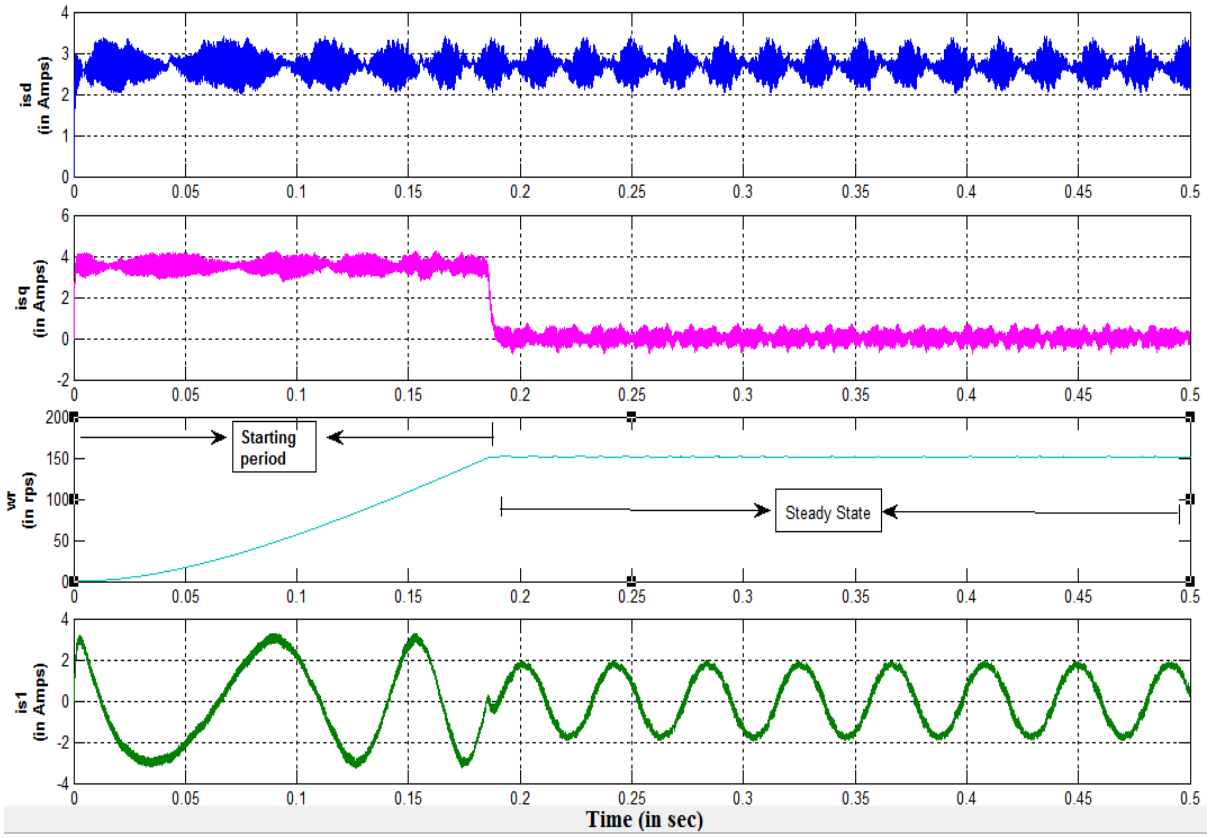

Fig 5.11: $i_{sd}, i_{sq}, w_r, i_{s1}$ plots showing starting & steady state characteristics

Fig-5.11 shows starting & steady state characteristics of various entities subjected to certain initial speed reference. During transient period, i_{sq} & i_{s1} are the rated maximum currents. The moment speed reaches the applied speed reference, i_{sq} & i_{s1} come down to its no-load values. i_{sd} keeps constant at the given reference value.

(6) Fig-5.12 shows characteristics of various entities when a negative speed reference is applied to the system. We can clearly observe the current reversal in the stator current i_{s1}- waveform.

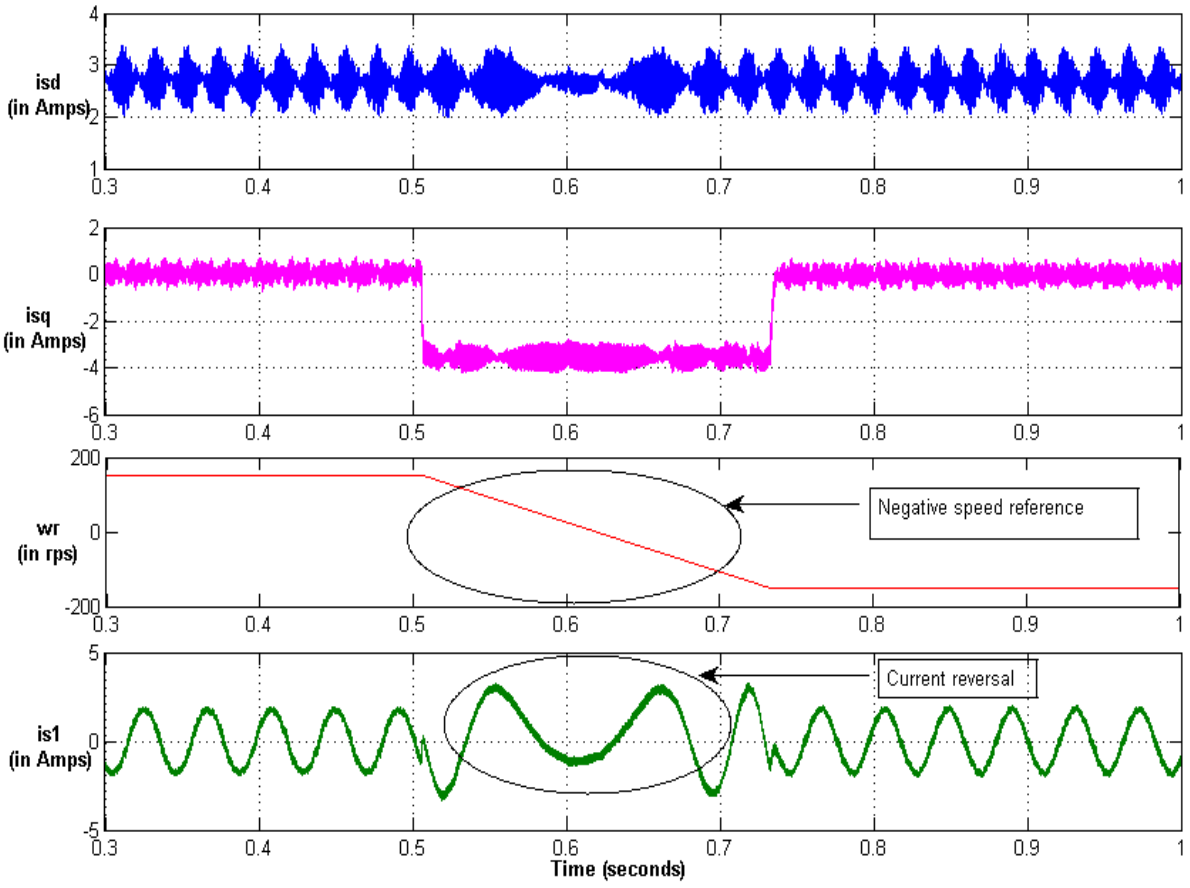

Fig 5.12: $i_{sd}, i_{sq}, w_r, i_{s1}$ - plots when subjected to negative speed reference

CHAPTER 6

HARDWARE IMPLEMENTATION & RESULTS:

6.1. FINDING MOTOR PARAMETERS:

A 3-phase star connected, squirrel induction motor was used for the project. The rotor shaft was provided with drum & belt arrangement for loading application. The name plate specifications are as follows:

Table 6.1: Name plate Specifications

Power (in Watt)	750
line to line Voltage (in volt)	415 Volt
Current (in ampere)	1.8 Amp
Power factor (cos ϕ)	0.81
Mechanical speed (in rpm)	1395
Frequency (in Hz)	50
Pole	4

Apart from these specification, we need other parameters such as rotor & stator resistances (Rr, Rs), rotor & stator self-inductances (Llr, Lls), mutual inductance (Lo), moment of inertia (J), friction co-efficient (B) for vector control scheme. The circuit model for induction motor is as follows:

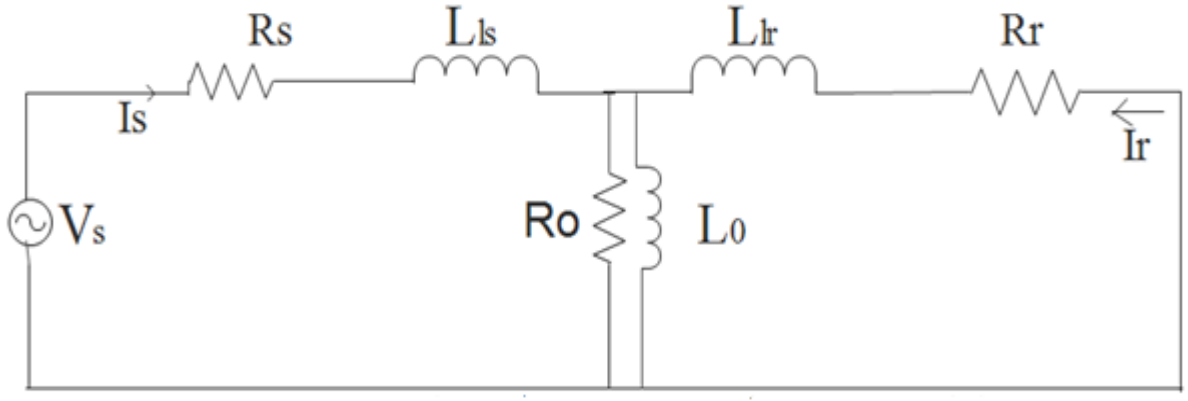

Fig 6.1: Equivalent circuit for induction motor at steady state

So various tests such as stator resistance test, open circuit test (OC), Blocked rotor test, retardation test etc. had been conducted to find out all motor parameters.

6.1.1 Stator resistance measurement:

Stator resistance was found out to be **13.5 ohm/ phase** from applied DC voltage and resulting current.

6.1.2. Open Circuit (No load) test:

As the induction motor & transformer's equivalent circuits are quite similar, same tests are performed to determine the circuit parameters such as OC & SC tests.

In open circuit test, rated voltages were applied to the stator terminals at the rated frequency with the rotor uncoupled from any mechanical load (motor spins freely). Current, voltage and power are measured at the motor input side. The losses in the no-load test are those due to core losses, winding losses, wind age and friction. Motor will rotate at almost synchronous speed because the slip is very small.

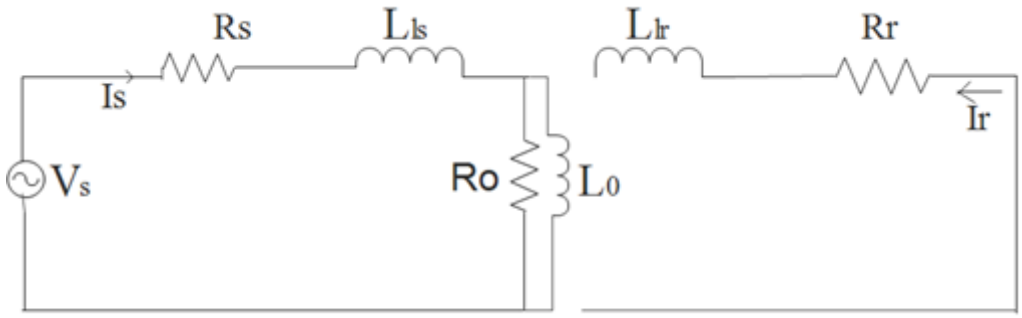

Fig 6.2: Equivalent circuit for Open circuit test

The values of voltage (v), current (i) & power (P) got from oscilloscope were 630 volt (p-p), 4.55 amps (p-p), 72 watt respectively.

$$\cos \emptyset = \frac{P}{V_{ph} * i_{ph}}$$

$$= \frac{72}{(\frac{630}{2}/\sqrt{2}) * (\frac{4.55}{2}/\sqrt{2})} = 0.201$$

$$i_m = i_o \sin \phi = 1.5758$$

$$i_c = i_o \cos\phi = 0.32334$$

$$R_c = \frac{V}{i_c} = 688.86\ ohm$$

$$L_m = \frac{V}{i_m * 2 * \pi * f} = 450.157\ mH$$

6.1.3. SC test (Blocked rotor test):

In this test, rotor was locked by brake drum and belt arrangement. A three phase AC voltage is applied gradually by an autotransformer to an appropriate value, so that the current of each phase is equal to its rated value i.e. 1.8 amps (phase value). Input power (p), voltage (v), current (i), was measured by an oscilloscope & noted down. Since the rotor is in stand-still condition the slip of the motor in this condition is 1 (s=1). The following reading were got from the locked rotor test, voltage =149 volt (p-p), current= 5 amps (p-p), power= 73.76 watt.

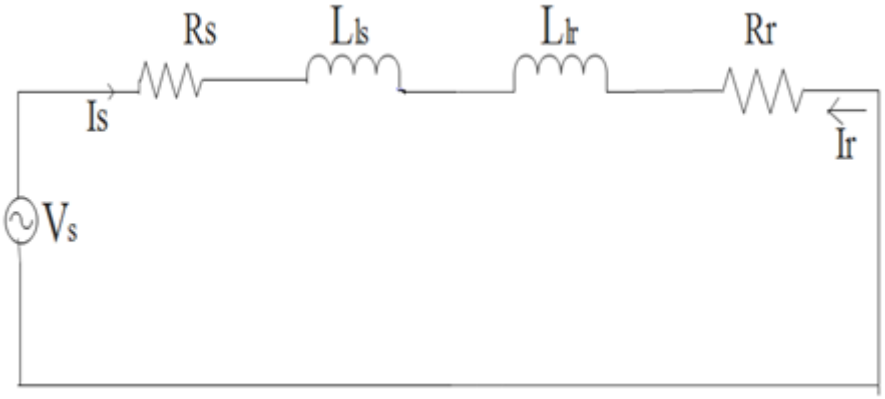

Fig 6.3: Equivalent circuit for Short circuit (Locked rotor) test

$$\cos\emptyset = \frac{P}{V_{ph} * i_{ph}}$$

$$= \frac{73.76}{(\frac{149}{2}/\sqrt{2}) * (\frac{5}{2}/\sqrt{2})} = 0.792$$

$$Z_{sc} = \frac{Vsc}{i_{sc}} = 29.8\ ohm$$

$$R_r = Z_{sc} \cos\phi - R_s = 29.8 * 0.792 - 13.5 = 10.101\ ohm$$

$$X_{eq} = Z_{sc} \sin\phi = 18.1935$$

$$X_{eq} = X_{lr} + X_{ls}$$

Again taking $X_{ls} = X_{lr}$, $X_{ls} = X_{lr} = \frac{X_{eq}}{2}$

So $L_{ls} = L_{lr} = \frac{(\frac{X_{eq}}{2})}{2*\pi*f}$ =28.97 mH

6.1.4. Retardation Test:

In this test, the machine is speeded beyond its rated speed without any load & then supply is cut from the source. The rotor speed slows down to zero speed & its kinetic energy is utilized to meet rotational losses i.e. frictional and windage losses.

During this process motor speed was measured w.r.t time and plotted in graph paper.

Kinetic energy of the rotor (E) = ½ J * w^2 (where w = angular velocity)

$$\frac{dE}{dt} = \frac{1}{2} * J * 2w * \frac{dw}{dt}$$

$$\text{Power } P = \frac{dE}{dt} = J * w * \frac{dw}{dt}$$

Taking $w = \frac{2*\pi*N}{60}$, Power $P = 0.01096 * J * N * \frac{dN}{dt}$

Different speeds w.r.t time got from this experiment is given below:

Table 6.2: Speed & time values for Retardation test

Speed (rpm)	Time (sec)
1448.85	0
1081.16	6.3
715.83	13.97
519.98	18.56
411.69	21.69
0	38.27

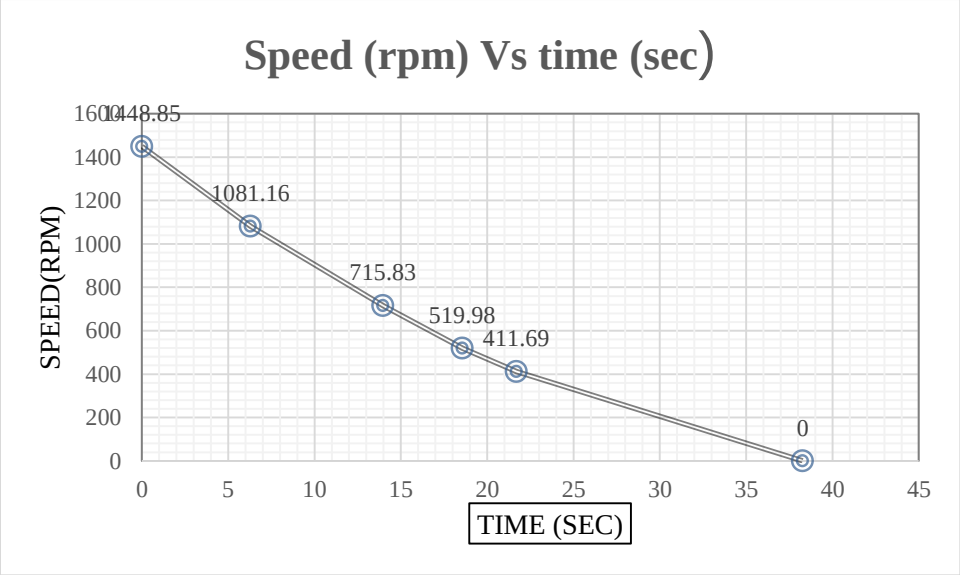

Fig 6.4: Speed Vs Time curve for retardation test

So from above Fig $\frac{dN}{dt} = slope\ of\ the\ curve = \frac{1220}{32.55} =$ 37.481

$$\text{Now P} = 0.01096 * \text{J} * \text{N} * \frac{dN}{dt}$$

$$\text{So J} = \frac{P}{0.01096 * \text{N} * \frac{dN}{dt}}$$

$$= \frac{72}{0.01096 * 1500 * 37.481}$$

$$= 0.11684 \text{ kg-m}^2$$

All parameters calculated from above tests are listed below:

Table 6.3: Calculated Motor parameters

$\boldsymbol{R_s}$	13.5 Ohm
$\boldsymbol{R_r}$	10.101 Ohm
$\boldsymbol{R_m}$	688.86 Ohm
$\boldsymbol{L_{ls}}$	28.97 mH
$\boldsymbol{L_{lr}}$	28.97 mH
$\boldsymbol{L_m}$	450.157 mH
J	0.11684 Kg-m2

6.2. SPEED DETECTOR:

To detect the speed of the motor, an infrared emitting diode and photo-transistor H21A1 is fitted to the body. The motor brake drum consists of 14 teeth or slots.

The H21A1 speed sensor consists of a gallium arsenide infrared emitting diode coupled with a silicon phototransistor in a plastic housing. The packaging system is designed to optimize the mechanical resolution, coupling efficiency, ambient light rejection, cost and reliability. The gap in the housing provides a means of interrupting the signal with an opaque material, switching the output from an "ON" to an "OFF" state.

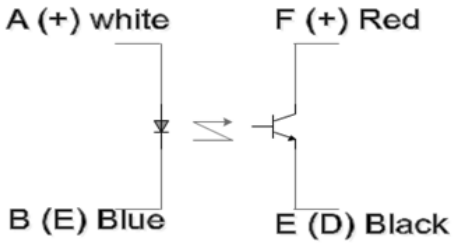

Fig 6.5: Speed Encoder-H21A1

H21A1 is mounted on the motor body so that when motor rotates, the slots mounted the brake drum interrupts the light, hence a digital pulse is generated from the transistor from which speed can be calculated from the time period (T_{slot}) of on-off pulse.

So motor speed can be calculated from the formula: **N (rpm) = 60 / (14* T_{slot})**

Circuit Connection diagram:

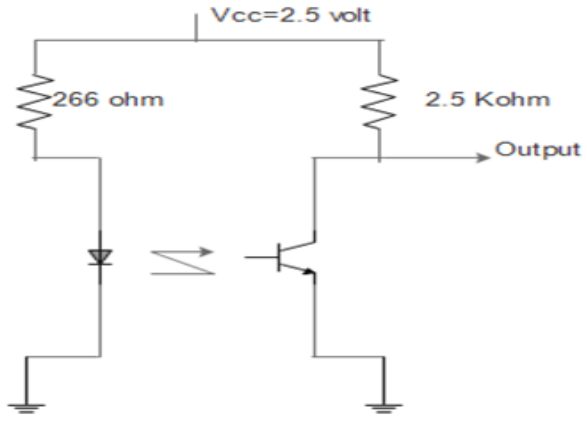

Fig 6.6: Connection diagram for H21A1

6.3. DIGITAL PLATFORM SELECTION:

To implement vector control, the evaluation board has to have certain characteristics to support the complexity of the control scheme, these characteristics are listed below:

1-ADC input requirement & speed of conversion:

We need at least 4 ADC input channels, two for current, one for DC link voltage & one for sampling of speed signal.

ADC conversion is expected to be less than one tenth of the PWM switching period. If PWM switching period is 100 microseconds, the ADC conversion time should be less than 10 microseconds.

2- Three phase PWM

Three pairs of PWM triggering signals required with a switching frequency in range of 10 KHz. Again the PWM resolution (no of bits used by counter) should be at least 12-bit.

3- System clock frequency or counter frequency:

To support a carrier wave of 10 KHz, the system clock frequency should be more than 81 MHz.

4- On board Programming: The emulator should be of superior capacity to support programming, debugging and downloading.

5- Cost: DSP board should be cost effective.

After comparing all these aspects of various boards**, dSPACE DS1104 board** is selected & used in this project.

6.4. HARDWARE SETUP

- A 1.1 Kw induction motor was used for vector control implementation. A DC-generator is coupled with the induction motor for loading purpose.
- The Inverter-Bridge is made up of **SEMIKRON-SKM 100GB128D IGBTS** with **SKYPER 32R** driver & adapter card.
- The DC-bus voltage is raised up to **200 V** instead of 650V due to hardware limitation.
- A protection board is used to limit three phase currents & DC-bus voltage.

- A rotary encoder (**AUTONICS E40H8-2000-6-L-5)** is used to give speed feedback to the machine.
- **LA-55A & LV25 LEM**-Sensors are used for current sensors and DC bus voltage sensors.
- We control the start-stop-restart options of the control algorithm from the PC (computer). We can change various reference values, controller parameters from the PC.
- The switching frequency of the inverter is set at **5 KHz**.
- A CRO is connected to observe & record various waveforms.

The schematics of the hardware setup is shown in Fig-6.7 & a close view of the prototype used is shown in Fig-6.8 & Fig-6.9.

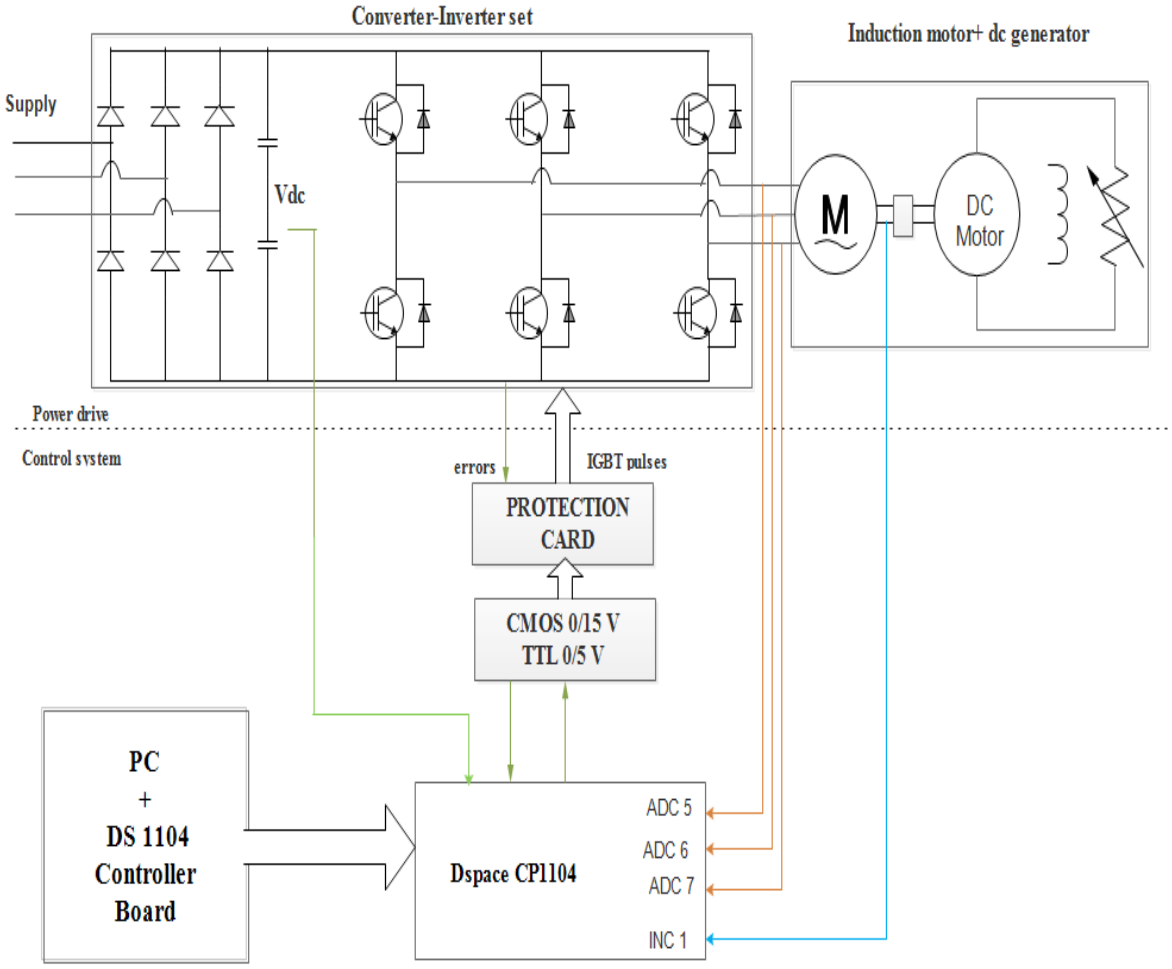

Fig 6.7: Hardware Setup

Experimental setup pics:

Fig 6.8: Experimental setup for 2-levl-inverter fed 3 phase induction motor

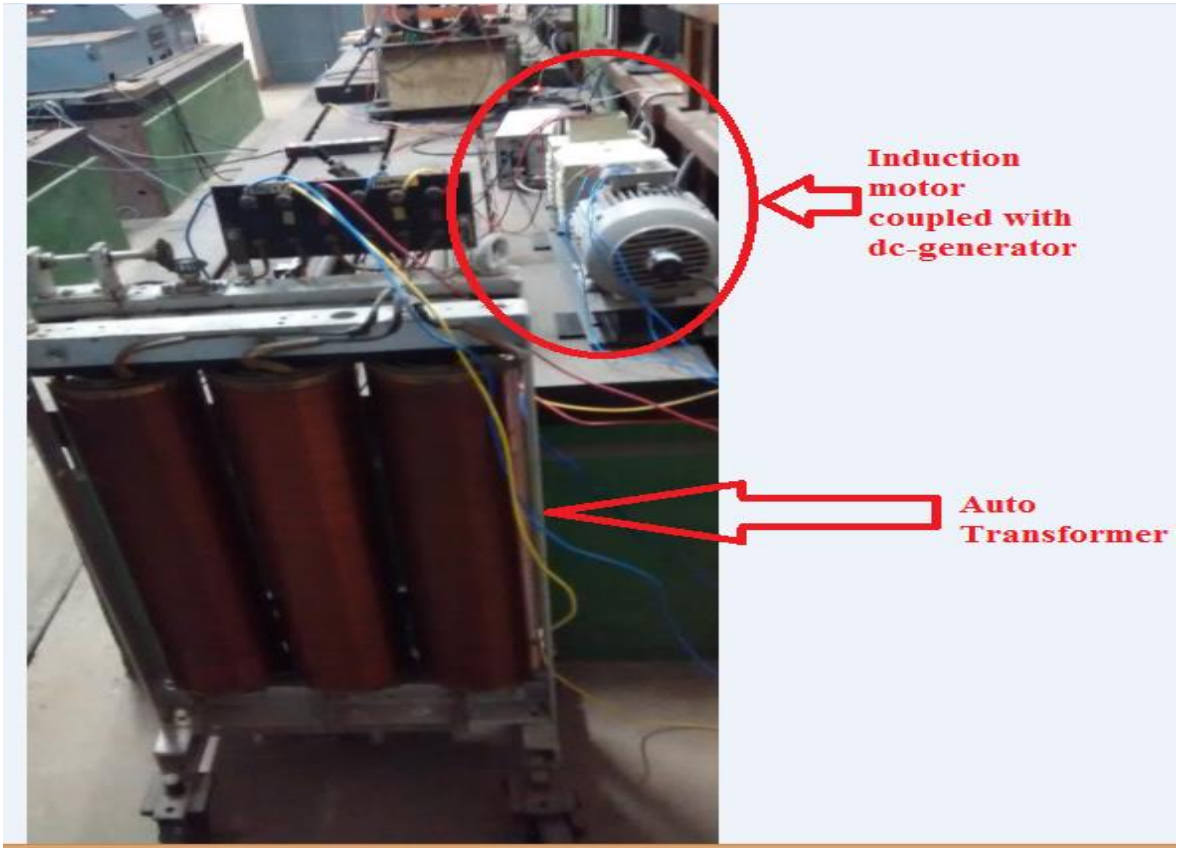

Fig 6.9: Close view of Autotransformer & motor-dc generator coupling

6.5. BASIC FEATURES & SPECIFICATION OF dSPACE DS1104 board

This section defines the list of supported inputs and outputs and features on the dSPACE DS1104 board. It give details on each feature and input and output in the dSPACE DS1104 R&D Controller Board Features.

Main Processor:

- MPC8240, PowerPC 603e core, 250 MHz
- 32 Kbyte internal cache

Timers

- 1 sample rate timer, 32-bit down counter
- 4 general purpose timers, 32 bit
- 64-bit time base for time measurement.

Memory:

- 32 Mbyte synchronous DRAM (SDRAM)
- 8 Mbyte boot flash for applications

Mux ADC Unit

1 A/D converter (ADC1) multiplexed to four channels (signals ADCH1 … ADCH4).The input signals of the converter are selected by a 4:1 input multiplexer. The A/D converters have the following characteristics:

- 16-bit resolution
- ±10 V input voltage range
- ± 5 mV offset error
- ± 0.25% gain error
- 80 dB (at 10 kHz) signal-to-noise ratio (SNR)

These inputs are used in polling mode.

The end of A/D conversion interrupt and the synchronized start of A/D conversion are not supported. The application range is the same as the voltage range: -10…..10 .

Parallel ADC Converters

4 parallel A/D converters (ADC2 … ADC5) with one channel each (signals ADCH5 … ADCH8). The A/D converters have the following characteristics:

- 12-bit resolution
- ±10 V input voltage range
- ± 5 mV offset error
- ± 0.5% gain error
- 70 dB signal-to-noise ratio (SNR)

These inputs are used in polling mode.

In case more than one channel is used, all the channels are read at the same time.

The end of A/D conversion interrupt and the synchronized start of A/D conversion are not supported. The application range is the same as the voltage range: -10..10.

DAC Unit

The master PPC on the DS1104 controls a D/A converter. It has the following characteristics:

- 8 parallel DAC channels (signals DACH1 … DACH8)
- 16-bit resolution
- ±10 V output voltage range
- ± 1 mV offset error, 10 µV/K offset drift
- ± 0.1% gain error, 25 ppm/K gain drift
- 80 dB (at 10 kHz) signal-to-noise ratio (SNR)
- Transparent and latched mode

The following parameters can be defined independently for each channel

- Initial value
- Termination value: hold the last value of the application or termination value specified by the user. The synchronized update of the DAC is not supported.

The application range is the same as the voltage range: -10..10.

Bit I/O Unit

The master PPC on the DS1104 controls a bit I/O unit with the following characteristics:

- 20-bit digital I/O
- Direction selectable for each channel individually
- ±5 mA maximum output current
- TTL voltage range for input and output

The following parameters can be defined independently for each channel

- Input our output mode
- Initial value
- Termination value: hold the last value of the application or termination value specified by the user.

Incremental Encoder Interface

The master PPC on the DS1104 controls an incremental encoder interface. It has the following characteristics:

- Input channels for two digital incremental encoders
- Support of single-ended TTL and differential RS422 signals
- 24-bit position counter
- 1.65 MHz maximum encoder line count frequency.
- Line termination for differential inputs
- Power supply for incremental encoders (5V and 0.1A)
- 5 V / 0.5 A sensor supply voltage

The following parameters can be defined independently for each channel

- TTL or RS422 mode
- Reset on index mode: true or false
- Initial position

A line subdivision of 4 is used. This configuration cannot be changed. The synchronized incremental encoder position strobe is not supported.

PWM Generation

The slave DSP provides four output channels for 1-phase PWM signal generation. The PWM mode (asymmetric or symmetric) and the PWM period can be specified globally for the four channels.

The minimum and maximum periods depend on the mode:

• Symmetric mode: period between 100 ns and 400 ms

• Asymmetric mode: period between 200 ns and 800 ms

The following parameters can be defined independently for each channel

• Polarity (active high or active low)

• Initial duty cycle

• Termination duty cycle: hold the last value of the application or termination value specified by the user.

Conflicting I/O features when using D2F channel 4, you cannot generate standard PWM signals.

3-Phase PWM Generation

The slave DSP provides 3 output channels (phases) for 3-phase PWM signal generation (PWM3) in the frequency range 1.25 Hz … 5 MHz

PWM3 signals are centered on the middle of the PWM period (symmetric mode). The polarity of the non-inverted PWM3 signals is active high. The period and dead band can be specified globally.

The following parameters can be defined independently for each channel (i) Initial duty cycle, (ii) Termination duty cycle- It can hold the last value of the application or termination value specified by the user. The PWM interrupt is not supported.

Physical Characteristics

- Power supply 5 V, 2.5 A / -12 V, 0.2 A /12 V, 0.3 A
- Requires one 32-bit PCI slot

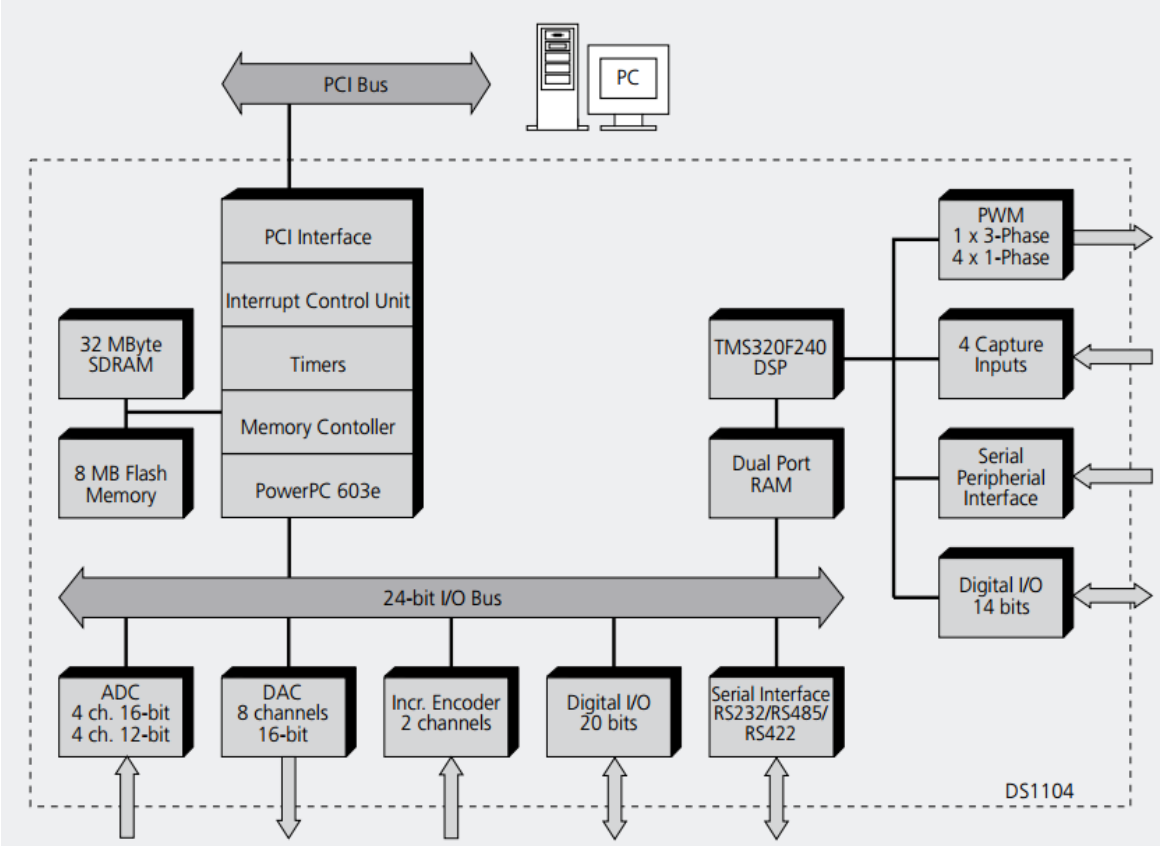

Fig 6.10: DS1104 R&D Controller Board

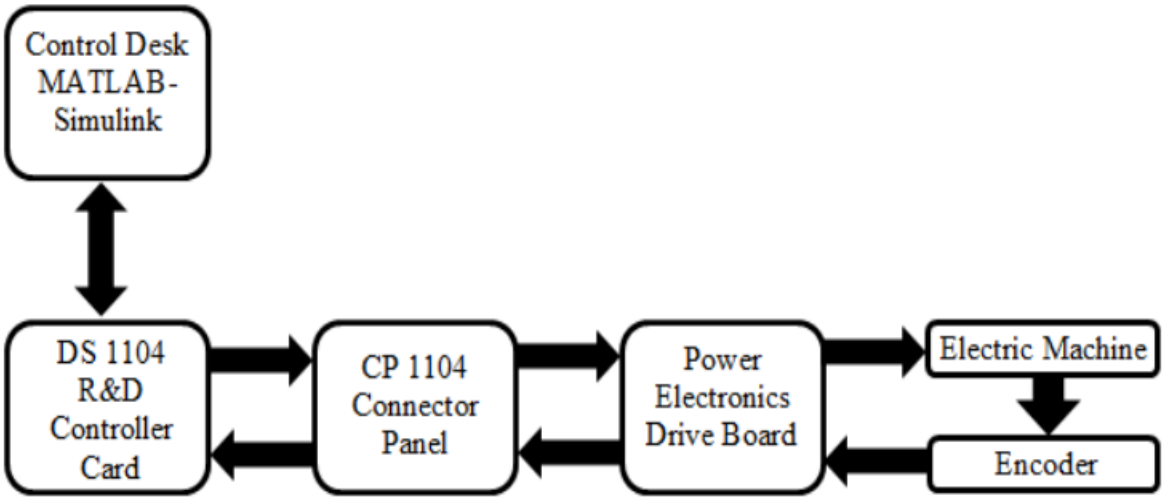

Fig 6.11: DSpace setup Block Diagram

6.6. ADC SIGNALS' INTERFACING

In Simulink, an analog-to-digital channel block dragged and dropped from >>Simulink Library Browser > dSPACE RTI1104 > DS1104 MASTER PPC >

DS1104ADC_C5/C6/C7/C8. The number of this channel can be changed similar to the digital-to analog-channel. There are a total of 8 ADCH channels on the I/O board, of which the last four can be accessed through this block by changing the port number. The first four channels are multiplexed and can be accessed through >>Simulink Library Browser > dSPACE RTI1104 > DS1104 MASTER PPC > DS1104MUX_ADC.

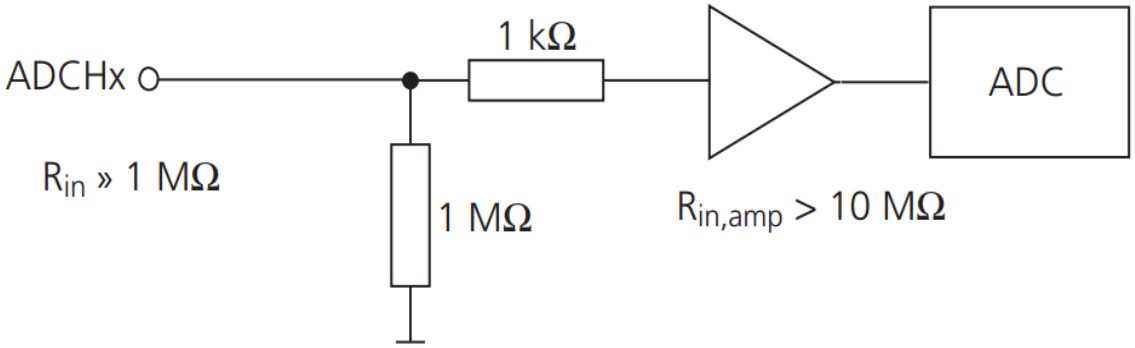

Fig 6.12: diagram of the input circuitry of the ADCs in dSpace

It is important to understand the "scaling" that occurs in acquiring the signal. The physical input signal input range is –10V to +10V. dSPACE always scales this by a factor of 0.1 (multiplies by this number) to place the value on a range of –1V to +1V. This scaling typically needs to be corrected for due to the need to map the meaning of volts to current in Amps. This mapping depends on sensor characteristics, and is generally adjusted in Simulink blocks when the sensor signal is processed before it is used by the main part of the controller.

We need to take the ADC signal and **multiply by 10** to remove the scale factor.

(i) Current Sensors

A **LEM-current Transducer LA 55-P (data sheet is given in Appendix-A)** is used for current sensing. It has various features such as:

- Excellent accuracy
- very good linearity
- Low temperature drift
- Optimized response time
- Wide frequency bandwidth
- High immunity to external interference
- Current overload capability.

Its primary nominal RMS current rating 50A & secondary maximum nominal RMS current is 50 mA. By using proper signal conditioning circuit, the primary to secondary transformation is 50 / **(7.5*5**).

Now multiply with ADC gain 10, the total gain for the ADC will be **(10*50) / (7.5 * 5).**

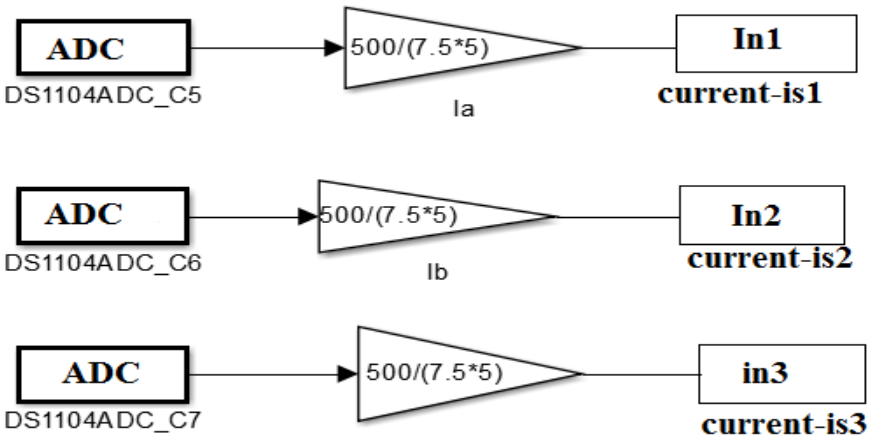

Fig 6.13: Simulink model of ADCs' interfacing for dSpace (currents)

(ii) Voltage Sensors

A **LEM-Voltage Transducer LA 55-P (data sheet is given in Appendix-B)** is used for voltage sensing. For voltage measurements, a current proportional to the measured voltage must be passed through an external resistor R1 which is selected by the user and installed in series with the primary circuit of the transducer.

The primary nominal RMS voltage is 500 V & the secondary maximum voltage is 6 V. Now multiplying ADC gain of 10, the total gain will be **(10 * 500) / 6**.

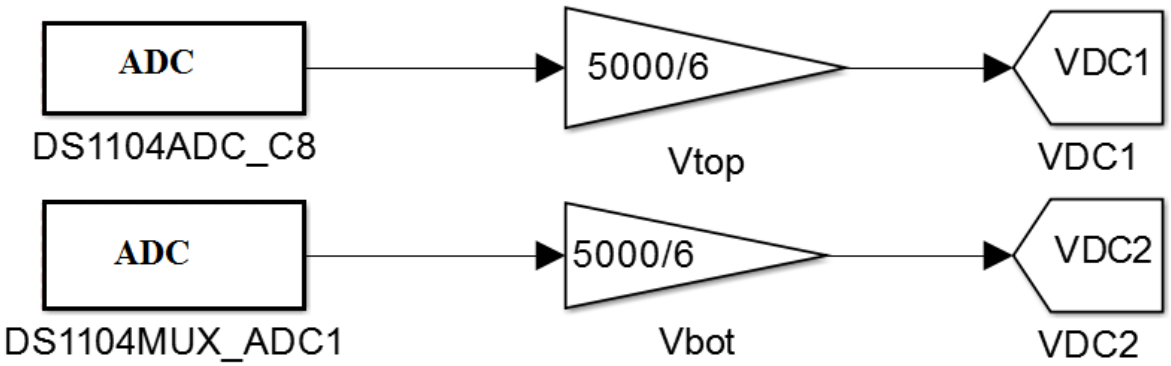

Fig 6.14: Simulink model of ADCs' interfacing for dSpace (Voltages)

6.7. SPEED ENCODER INTERFACING

A rotary encoder is mounted on the induction motor. The encoder position block can be found:

>>Simulink Library Browser > dSPACE RTI1104 > DS1104 Master PPC> DS1104ENC_POS_C1.

This block provides read access to the position and delta position of the two encoder interface channels. Also an **Encoder Master Setup** is added to the model. This block sets the global specifications for the channels of the encoder interface.

>>Simulink Library Browser > dSPACE RT11104 > DS1104 Master PPC> DS1104ENC_SETUP.

The encoder signal type in the encoder master setup block is set to single ended (TTL).

>> Double click > DS1104ENC_SETUP > Encoder signal type > Type> single ended (TTL).

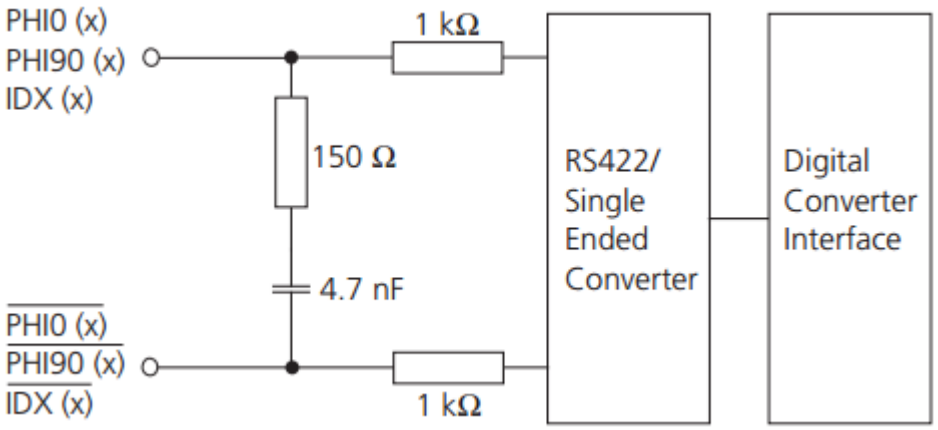

Fig 6.15: input circuitry of the digital incremental encoders.

The rotary encoder (E40H8-2000-6-L-5) used in this project is a hollow type with shaft diameter of 8 mm. The encoder consists of two thousand lines per-revolution, which is 0.18 degree-per-line. To convert the line count to degrees, the line count is multiplied by the constant 0.36. The encoder delta position output is used to compute the angular velocity of the machine in rad/sec by dividing it by the sampling time as in Fig 6.16.

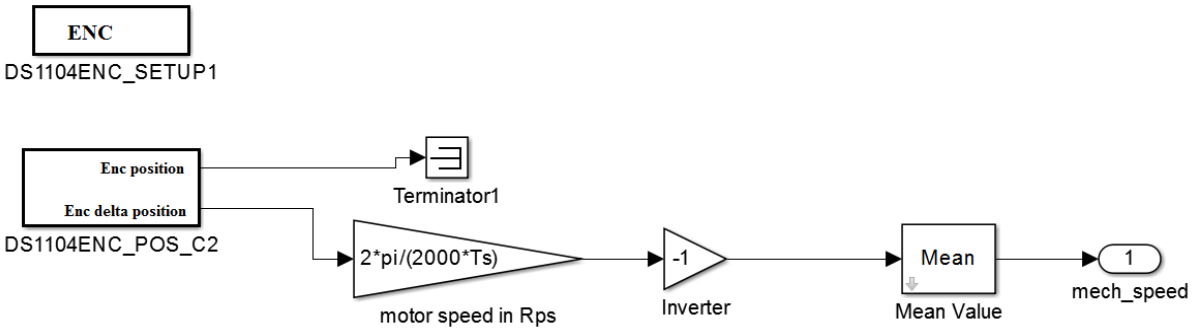

Fig 6.16: Encoder position and velocity read block

The inverter in Fig 6.16 is in place because the encoder for this system is mounted on the prime mover and not the generating machine. In order to obtain the correct position and speed values, the encoder data must be inverted. A "**Mean block**" is used to smooth the oscillation of the electric machines' captured velocity and filter out the noise. This block is shown in Fig 6.17 and it can be added to the model. The period in "Mean block" is 10 (n=10).

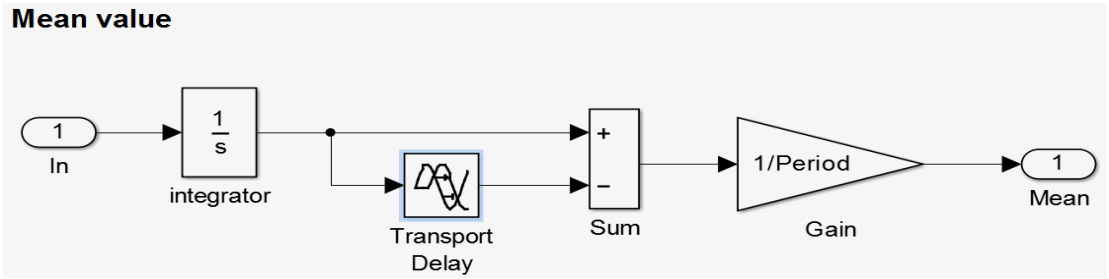

Fig 6.17: Mean block

6.8. DAC INITIALIZATION /TERMINATION

The DS1104 provides a digital/analog converter (DAC) with 8 parallel DAC channels. The analog output channels are called DACH1...DACH8**.** Channel Numbers are selected within the range 1 ... 8.

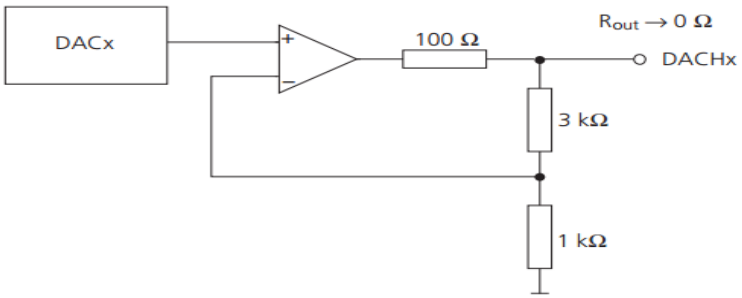

Fig 6.18: Diagram of the output circuitry of the DACs in dSpace

Since the output voltage range stays between -10 V to +10 V, Each entity is calibrated to this value. So to get actual result, we need to divide it by its unit value.

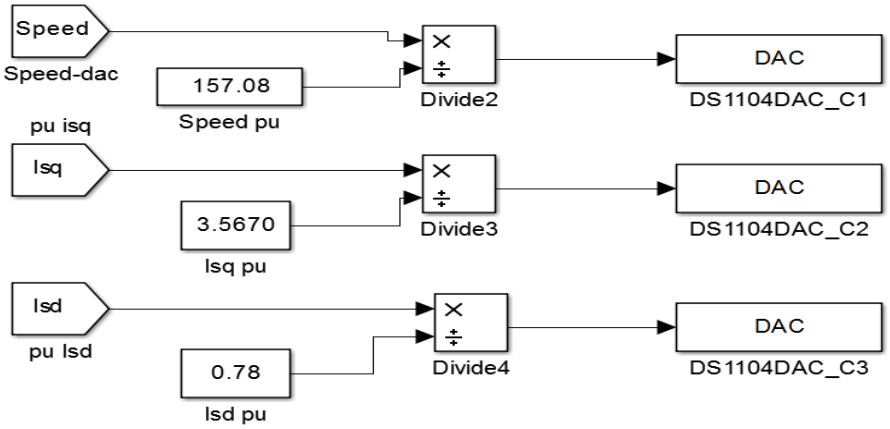

Fig 6.19: Simulink model for DAC for measurement of w_r, i_{sq}, i_{sd}

6.9. PWM PULSE INTERFACING IN DSPACE

The I/O inputs are converted to Boolean. This can be done with use of a Data Type Conversion found under Simulink **Library Browser > Simulink > Commonly Used Blocks > Data Type Conversion.** Change the output data type in this block to Boolean.

>> **Double click Data Type Conversion > Output data type > Boolean.**

Now that the I/O inputs are converted to Boolean, the signal can be sent to the control circuit with the use of a **slave bit out** block. This block can be found under Simulink Library Browser

>> **dSPACE RTI1104 > DS1104 SLAVE DSP > DS1104SL_DSP_BIT_OUT_C0.**

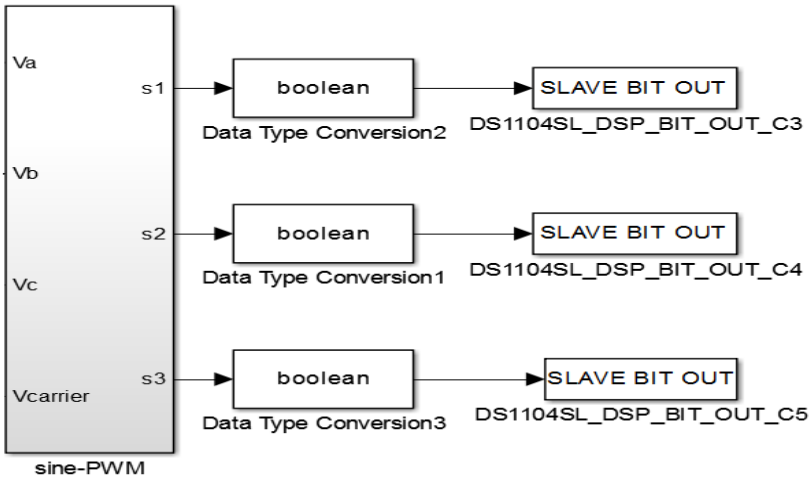

Fig 6.20: Simulink model for PWM pulses interfaced with dSPACE

Slave DSP Digital I/O:

The slave DSP of the DS1104 provides the following I/O: Slave DSP Bit I/O Unit, Slave DSP Timing I/O Unit, and Slave DSP Serial Peripheral Interface

The pins of the slave DSP digital I/O are called:

- SPWM1... SPWM9
- ST1PWM... ST3PWM
- SCAP1... SCAP4, SSOMI , SSIMO, SSTE & SSCLK

6.10. COMPLETE VC SIMULINK MODEL FOR DSPACE

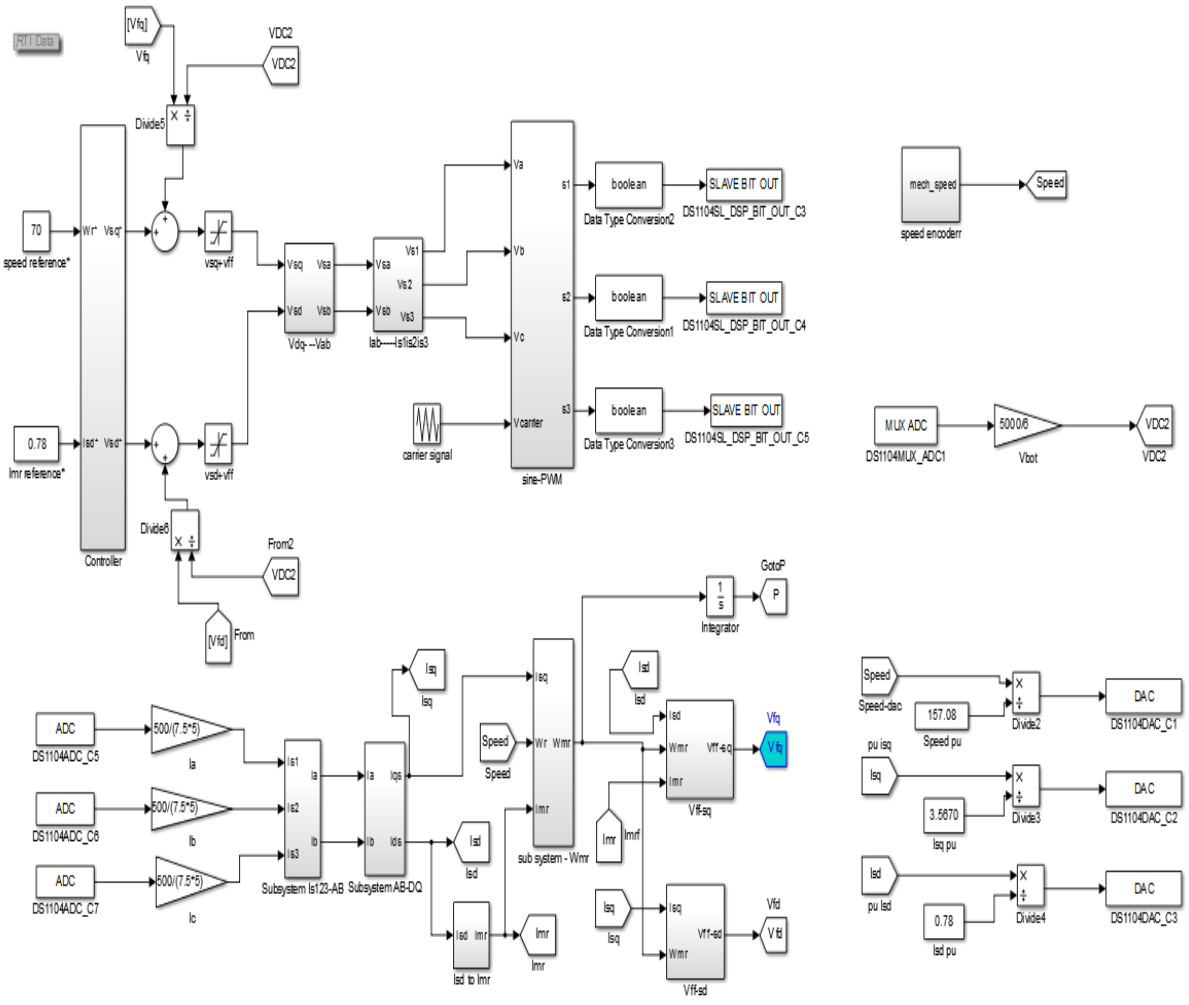

Fig 6.21: Full overview of Simulink model for vector control of an induction motor

Fig 6.21 shows the complete Simulink model for vector control. It consists of speed encoder block, ADC blocks, DAC blocks & PWM pulse blocks.

6.11. EXPERIMENTAL RESULTS & ANALYSIS

Expected Results: On application of "Vector Control Technique" to the induction motor

- The starting performance should be smooth.
- Machine should respond to speed reversal quickly without much oscillation.
- The torque response should be fast**.**
- The output current waveform should be sinusoidal without any harmonics.

6.11.1. Starting characteristics

We can see from Fig-6.22 that the moment gate pulses are given to the inverter i_{sd} jumps to its rated value & stays there without any disturbance, whereas i_{sq} jumps to its rated value & comes back to 0 when actual speed reaches the reference speed value. During Transient period there is maximum rated current flowing in the machine which suggests that the speed error is corrected at maximum torque (proportional to i_{sq}).

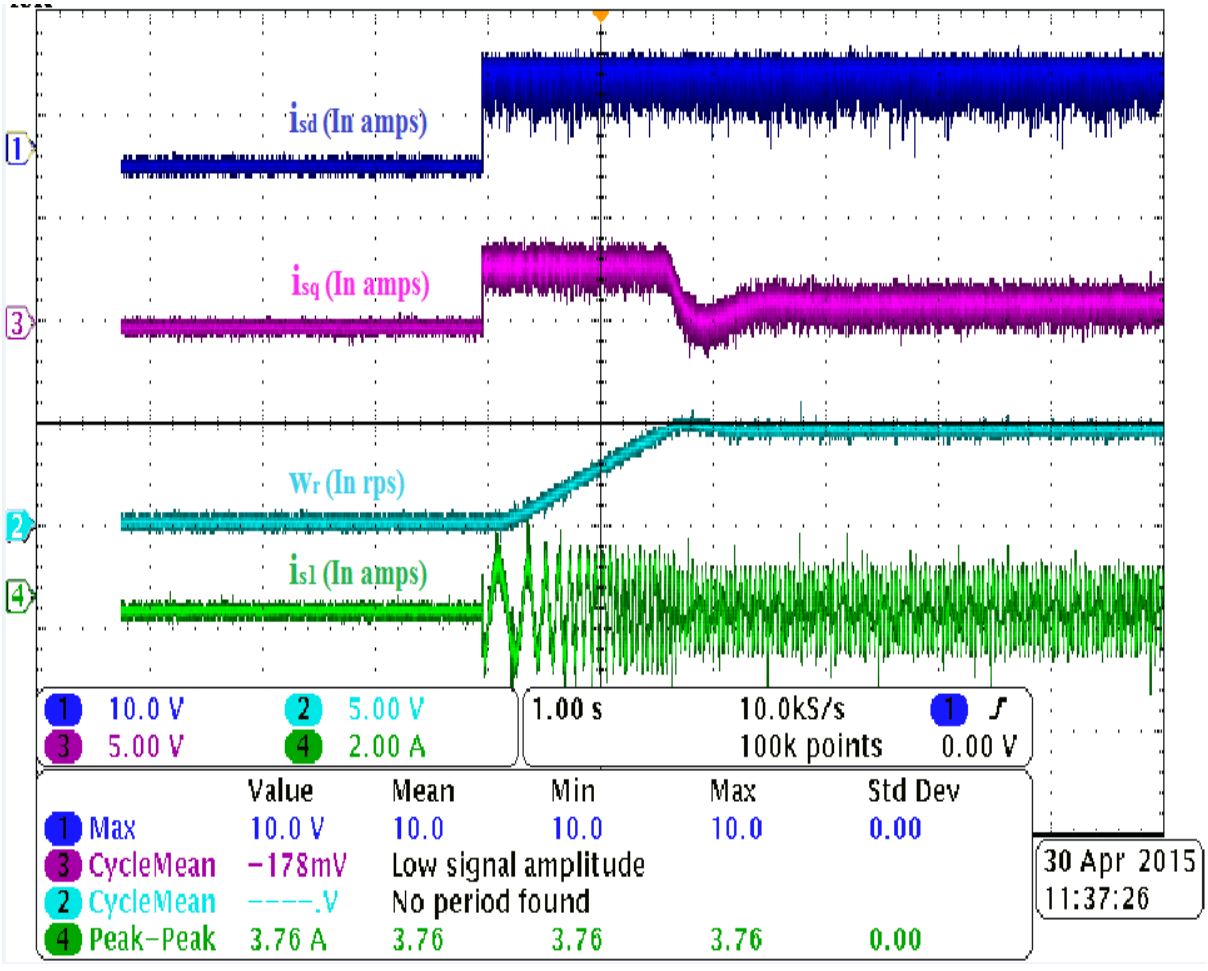

Fig 6.22: Starting response with a speed reference of 70 RPS (668.5 RPM)

6.11.2. Steady state characteristics

During steady state, the current flowing in the circuit depends on the load demand. From Fig-6.23, the output current to the motor is sinusoidal in nature although there some noise in the waveform. The speed response is just a straight line implying it is remaining constant. i_{sd} is constant at the set value where as there is some i_{sq} so as to support the no-load losses.

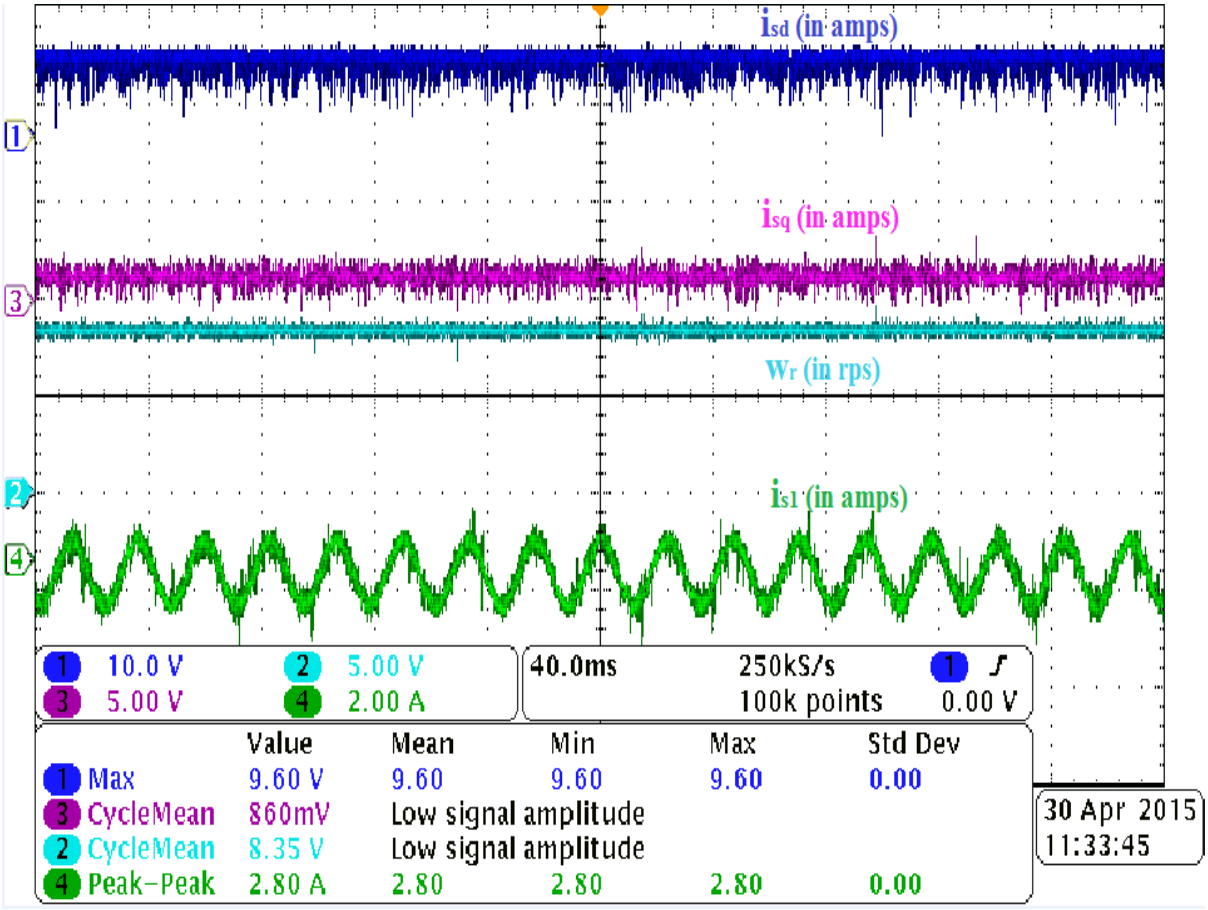

Fig 6.23: Steady state response with a speed reference of 70 RPS (668.5 RPM)

6.11.3. Speed reversal characteristics

Fig 6.24 shows the response of various entities when there is a negative step change in speed. The current is increased to its rated value during transient period, there is current reversal because of negative speed reference & finally it attains the steady state when speed reaches to the reference speed.

The i_{sd} - current remains constant because in vector control we keep the flux constant. The i_{sq} -current (corresponds to torque) drops down to its maximum negative value & comes to 0 again the moment actual speed reaches the reference speed.

Fig 6.25 shows transient response i_{sd} , i_{sq}, w_r, i_{s1} when there is a speed reversal from - ve value to a +ve value.

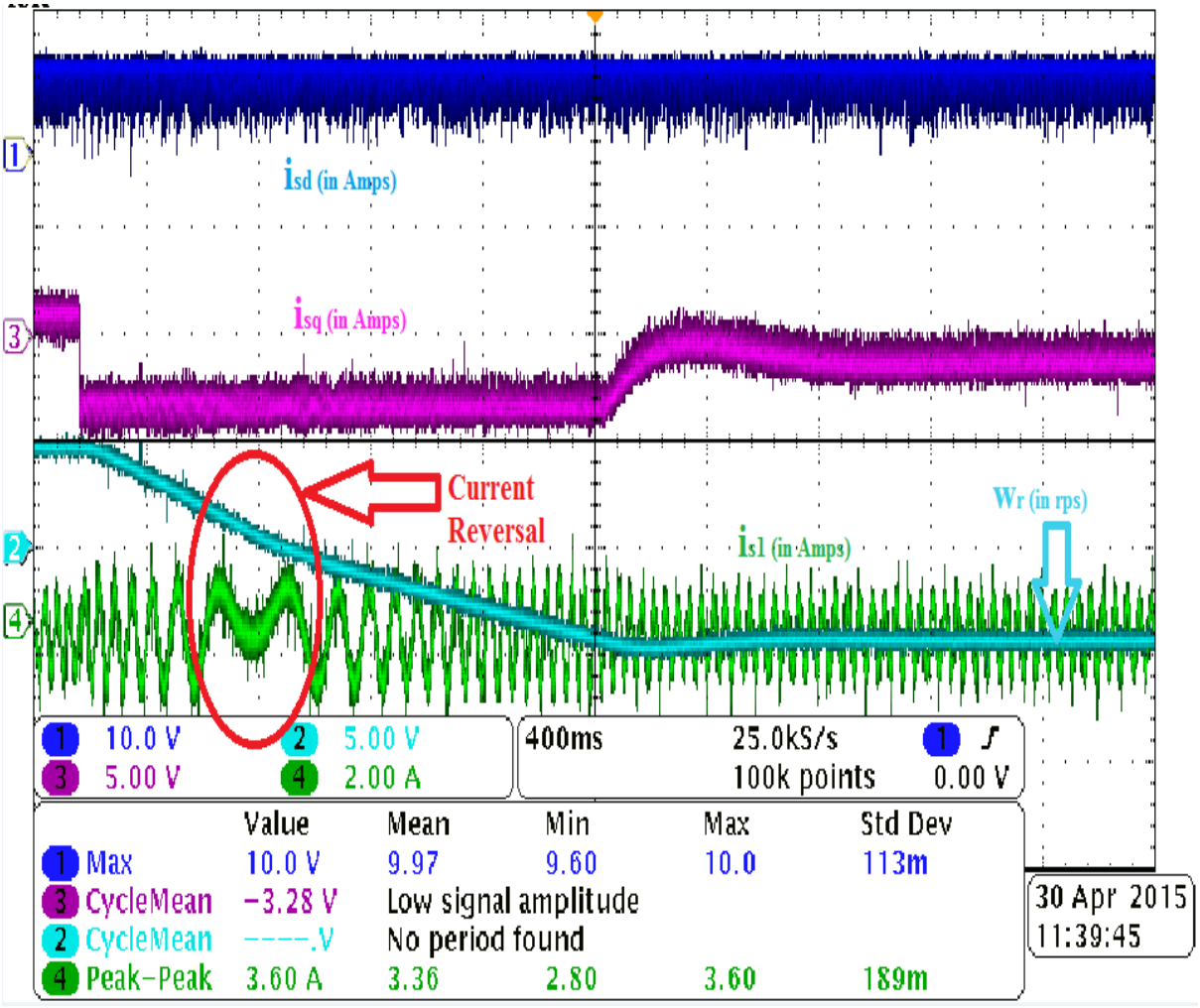

Fig 6.24: Transient response showing speed reversal from +70 to -70 RPS

6.11.4. Comparison of experimental results with simulation results:

Fig-5.11 in chapter-5 shows the simulation result of starting & steady state response of various entities. If we compare Fig-6.22 with Fig-5.11, we can see in both the figures during transient period i_{sq} & $i_{s1}(stator\ current)$ reaches its maximum rated current & the moment speed reaches the applied speed reference value(steady state condition), i_{sq} & i_{s1} come down to no-load values. i_{sd}-keeps constant at rated value irrespective of any disturbance in speed reference.

Fig-5.12 in chapter-5 shows the simulation result of various entities during negative speed reference. If we compare Fig-6.24 with Fig-5.12, there is a distinct current reversal in both the figure. So we can say that the experimental results are in close agreement with the simulation results.

CHAPTER-7

SUMMARY & CONCLUSION

7.1. SCOPE FOR FUTURE WORK

There remains a large potential to improve the performance of the present system. Since this thesis project is troubled by ADC noise a lot, the ADC conditioning circuit needs to be improved. More efforts can be put on circuit layout & PI controller design in future.

The problem of parameter variation can also be incorporated in this project. Some other control strategies could also be considered for regulator design in order to make the system less sensitive to the noise or the parameter variations. The current work is based on sensored speed feedback. We can also extend the research to analyze the sensor-less response of the system.

The output waveforms got from this project can also be improved by optimizing the controller parameters more. The waveforms got from this project can be compared with other speed control techniques available.

The inverter used in this project was hand-made. By using a properly designed inverter, the switching frequency can be increased up to 10 KHz, which in turn increases the speed of the response.

Space vector PWM (SVPWM) might be introduced into this control system to replace the SPWM, as it can reduce the harmonic distortion and is more efficient in the use of supply voltage.

7.2. SUMMARY & CONCLUSIONS:

In this project, basic principle of indirect field oriented control in rotor flux frame was studied with a three phase cage rotor induction motor. The model was simulated in MATLAB & results were analyzed. A two-level six-leg IGBT voltage source inverter (VSI) was used in the model controlled with sine-pwm (SPWM) firing technique. PI-controllers were used for speed, torque and flux control. The inverter switching frequency was set at 5 KHz whereas current controllers' bandwidth was set at 500 Hz and speed controller, flux controller's bandwidth was set at 50 Hz.

The purpose and objective of this project, mentioned in objective section in chapter-1 are fully achieved. The selection of the digital board is proved to be a success. The dSPACE DS1104

Control Platform facilitates and accelerates the hardware implementation part a lot. For the interface board part, the digital signal interfaces, such as PWM and incremental encoder, work satisfactorily.

The simulated model was used on a laboratory prototype system. DSPACE was used as digital platform to deal with complex calculation associated with the vector control technique. The experimental results are in close agreement with the simulated results. Experimental results showing the steady state and dynamic performance of the developed model are presented. The vector control system on the DSP manages to regulate the dq currents and the speed fast and accurately. The control coefficients in the PI regulators, k_i and k_p are optimized for the differences between the simulation and the experimental results.

This class of speed control drives are widely used in various industrial applications, and technology is continuously expanding. Vector control gives far better performance than V/f control or scalar control though it requires high speed DSP as its implementation with corresponding feedback signal estimation is complex in nature. This class of drive is also applicable for synchronous motors.

7.3. LIMITATIONS OF HARDWARE SETUP

- The maximum switching frequency given to the system was 5 KHz.
- The maximum DC voltage applied to the system was 200 V due to the hardware limitation.

APPENDIX A

Current Transducer LA 55-P (I_{PN}= 50 A):

For the electronic measurement of currents: DC, AC, pulsed..., with a galvanic isolation between the primary circuit (high power) and the secondary circuit (electronic circuit).

Electrical data

I_{PN}	Primary nominal r.m.s. current		50				A
I_P	Primary current, measuring range		0 .. ± 70				A
R_M	Measuring resistance @		T_A = 70°C		T_A = 85°C		
			$R_{M\,min}$	$R_{M\,max}$	$R_{M\,min}$	$R_{M\,max}$	
	with ± 12 V	@ ± 50 A_{max}	10	100	60	95	Ω
		@ ± 70 A_{max}	10	50	60[1)]	60[1)]	Ω
	with ± 15 V	@ ± 50 A_{max}	50	160	135	155	Ω
		@ ± 70 A_{max}	50	90	135[2)]	135[2)]	Ω
I_{SN}	Secondary nominal r.m.s. current		50				mA
K_N	Conversion ratio		1 : 1000				
V_C	Supply voltage (± 5 %)		± 12 .. 15				V
I_C	Current consumption		10 (@ ±15 V) + I_S				mA
V_d	R.m.s. voltage for AC isolation test, 50 Hz, 1 mn		2.5				kV

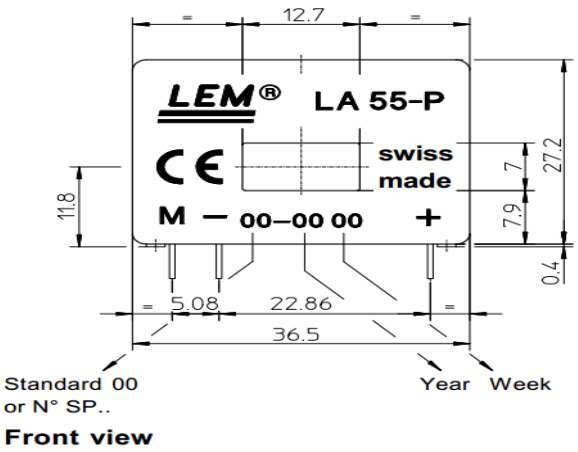

Front view

Secondary terminals

Terminal +: supply voltage + 12 .. 15 V

Terminal - : supply voltage - 12 .. 15 V

Terminal M : measure

Connection

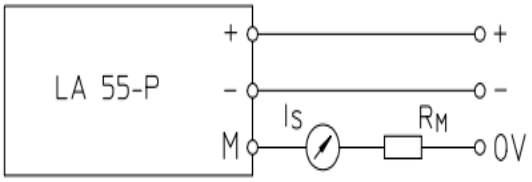

APPENDIX B

Voltage Transducer LV 25-P (I_{PN} = 10 mA, V_{PN} = 10 .. 500 V):

For the electronic measurement of voltages: DC, AC, pulsed..., with a galvanic isolation between the primary circuit (high voltage) and the secondary circuit (electronic circuit).

Electrical data

I_{PN}	Primary nominal r.m.s. current		10		mA
I_P	Primary current, measuring range		0 .. ± 14		mA
R_M	Measuring resistance		$R_{M\,min}$	$R_{M\,max}$	
	with ± 12 V	@ ± 10 mA $_{max}$	30	190	Ω
		@ ± 14 mA $_{max}$	30	100	Ω
	with ± 15 V	@ ± 10 mA $_{max}$	100	350	Ω
		@ ± 14 mA $_{max}$	100	190	Ω
I_{SN}	Secondary nominal r.m.s. current		25		mA
K_N	Conversion ratio		2500 : 1000		
V_C	Supply voltage (± 5 %)		± 12 .. 15		V
I_C	Current consumption		10 (@±15 V) + I_S		mA
V_d	R.m.s. voltage for AC isolation test [1], 50 Hz, 1 mn		2.5		kV

Principle of use:

For voltage measurements, a current proportional to the measured voltage must be passed through an external resistor R1which is selected by the user and installed in series with the primary circuit of the transducer.

Primary resistor R 1

The transducer's optimum accuracy is obtained at the nominal primary current. As far as possible, R1 should be calculated so that the nominal voltage to be measured corresponds to a primary current of 10 mA.

Connection

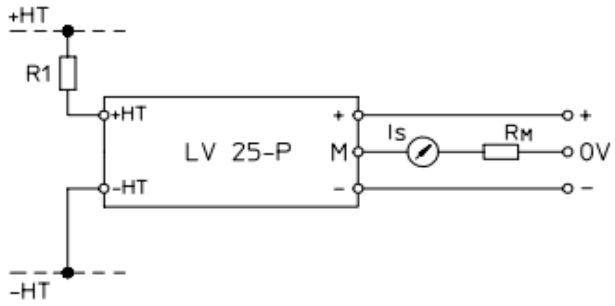

Secondary terminals

Terminal +: supply voltage + 12 .. 15 V

Terminal M: measure

Terminal - : supply voltage - 12 .. 15 V

REFERENCES

[1]. B.K.Bose,"Modern power electronics and AC drives."New Delhi, PHI Learning Private Limited, 2011.pp.413-408

[2]. W. Leonhard, "control of electric drives", Springer-Verlag, 1985

[3]. Krause, P.C.,Wasynczuk, O.& Sudhoff, S.D.Analysis of Electric Machinery, IEEE-1995

[4]. G.K. Dubey, "Fundamental of Electrical Drives", Narosa, 1994.

[5]. P. C. Krause, O. Wasynczuk, S. D. Sudhoff "Analysis of Electric Machinery and Drive Systems", IEEE Press, A John Wiley & Sons, Inc. Publication Second Edition, 2002.

[6]. Jun K. Kang, Jae T. Lee, Young LM. Kim, "speed controller design for induction motor drives"

[7]. "Pulse-width modulation," Web page, June 2011.
[Online]. Available: http://en.wikipedia.org/wiki/Pulse-width modulation

[8]. "Vector control (motor)," Web page, June 2011.
[Online]. Available: http://en.wikipedia.org/wiki/Vector control %28motor%29

[9]. A. Keyhani, "Pulse-width modulation (pwm) techniques," Department of Electrical and Computer Engineering, the Ohio State University, Tech. Rep.

[10].Santisteban, J. A. & Stephan, R. M. (2001). Vector control methods for induction Machines: an overview, IEEE Transactions on Education, vol. 44, no. 2, (May 2001), pp. 170-175, ISSN 0018-9359.

[11] "Ds1104 ppc controller board hardware reference," dSP ACE, Tech. Rep., March 2007